arXiv:1203.5634v2 [hep-ph] 28 May 2012

Local electric current correlation function in an exponentially decaying magnetic field

N. Sadooghi* and F. Taghinavaz†

Department of Physics, Sharif University of Technology, P.O. Box 11155-9161, Tehran-Iran

The effect of an exponentially decaying magnetic field on the dynamics of Dirac fermions in $3+1$ dimensions is explored. The spatially decaying magnetic field is assumed to be aligned in the third direction, and is defined by $\mathbf{B}(x)=B(x)\,\mathbf{e}_z$, with $B(x)=B_0e^{-\xi x/\ell_B}$. Here, ξ is a dimensionless damping factor and $\ell_B=(eB_0)^{-1/2}$ is the magnetic length. As it turns out, the energy spectrum of fermions in this inhomogeneous magnetic field can be analytically determined using the Ritus method. Assuming the magnetic field to be strong, the chiral condensate and the *local* electric current correlation function are computed in the lowest Landau level (LLL) approximation and the results are compared with those arising from a strong homogeneous magnetic field. Although the constant magnetic field B_0 can be reproduced by taking the limit of $\xi\to 0$ and/or $x\to 0$ from $B(x)$, these limits turn out to be singular, especially once the quantum corrections are taken into account.

PACS numbers: 11.15.-q, 11.30.Qc, 11.30.Rd, 12.20.-m, 12.20.Ds

I. INTRODUCTION

The effects of magnetic fields on systems containing relativistic fermions are subject of intense theoretical studies over the past two decades. These effects include a wide range, from condensed matter physics [1] to high energy physics [2] and cosmology [3]. Theoretical studies deal in the most of these works with the idealized limit of constant and homogeneous magnetic fields. However, this limit is only reliable as long as the scale of field variation is much larger than the Compton wavelength of the fermionic system. As it is shown in [4], strong and homogeneous magnetic fields lead to the formation of fermion bound states even in the weakest attractive interaction between the fermions. This phenomenon, known as magnetic catalysis of dynamical chiral symmetry breaking [5], is essentially based on a dimensional reduction from D to $D-2$ dimensions in the presence of strong homogeneous magnetic fields in the regime of LLL dominance. However, as it is demonstrated recently in [6], massless Dirac electrons can also be confined by inhomogeneous magnetic fields in graphene, which is a single layer of carbon atoms in a honeycomb lattice. Electrons in graphene are described by a massless two-dimensional, time-independent relativistic Dirac equation. As it is shown in [6], magnetic quantum dots can be formed, if one neglects the effects of electron spin and solves the Dirac equation in the presence of a square well magnetic barrier of width $2d$, $\mathbf{B}(\mathbf{x})=B(x)\,\mathbf{e}_z$, directed perpendicular to the graphene $x-y$ plane, with $B(x)=B_0\theta(d^2-x^2)$, and θ the Heaviside step function. A circularly symmetric magnetic quantum dot arises then by a radially inhomogeneous magnetic field $\mathbf{B}=B(r)\,\mathbf{e}_z$ (see [6, 7] for more details). In [8], the bound state solutions and the spectra of graphene excitations in the presence of an inverse radial magnetic field, with $B(r)\sim\frac{1}{r}$, is studied. Analytical solutions for the Dirac equation in the presence of double or multiple magnetic barriers are presented in [9]. The bound spectra of electrons in a magnetic barrier with hyperbolic profile is studied in [10].

In the present paper, we will focus, in particular, on the solution of Dirac equation in the presence of an exponentially decaying magnetic field. Analytical solution of a quasi-two-dimensional Dirac equation including the spin of a single electron in a magnetic field of constant direction with arbitrarily strong exponentially depending variation perpendicular to the field direction is firstly presented in [11]. In [12], the probability density and current distributions of Dirac electrons in graphene in the presence of an exponentially decaying magnetic field are determined. The formation of chiral condensate induced by exponentially decaying magnetic fields, in $2+1$ dimensions, is studied in [13]. The vacuum polarization tensor of 3+1 dimensional scalar Quantum Electrodynamics in the presence of an inhomogeneous background magnetic field, arising from a general plane wave basis for the underlying gauge field, is computed recently in [14]. In order to demonstrate the *nonlocal* features of quantum field theory in the presence of inhomogeneous background magnetic fields, the vacuum polarization tensor is defined to be *local*. This turns out to be a useful task providing *local* information about the *nonlocal* nature of fluctuation-induced processes [14]. In the present paper, following the same idea as in [14], we will de-

---

*Electronic address: sadooghi@physics.sharif.ir
†Electronic address: taghinavaz@physics.sharif.ir

fine a *local* electric current correlation function (local electric susceptibility), and compute it in the presence of a strong and exponentially decaying magnetic field in the LLL approximation. Eventually, we will compare the result with the electric current correlation function arising from a strong homogeneous magnetic field and discuss the effects of inhomogeneity of the background magnetic field.

The organization of the paper is as follows: In Sec. II A, we will briefly review the Ritus eigenfunction method [15] by solving the Dirac equation in the presence of a constant and homogeneous magnetic field. In Sec. II B, we will introduce an exponentially decaying magnetic field $\mathbf{B}(x) = B(x)\mathbf{e}_z$, which is assumed to be aligned in the third direction, with $B(x)$ given by $B(x) = B_0 e^{-\xi x/\ell_B}$. Here, ξ is a dimensionless damping parameter and $\ell_B = (eB_0)^{-1/2}$ is the magnetic length. Using the Ritus method, the energy eigenvalues and eigenfunctions of a $3+1$ dimensional Dirac equation in the presence of $\mathbf{B}(x)$ will be determined. In Sec. III, we will determine the chiral condensate $\langle\bar{\psi}\psi\rangle$, using the fermion propagator in the presence of strong homogeneous (Sec. III A) and exponentially decaying magnetic fields (Sec. III B) in the LLL approximation. We will show that whereas $\langle\bar{\psi}\psi\rangle$ in a strong homogeneous magnetic field is constant, $\langle\bar{\psi}\psi\rangle$ in an exponentially decaying magnetic field depends nontrivially on a dimensionless variable u, defined by $u = \frac{2}{\xi^2} e^{-\xi x/\ell_B}$. In Sec. IV, the local electric current correlation function (local electric susceptibility) $\chi^{(i)}$ will be computed in the presence of strong homogeneous (Sec. IV A) and exponentially decaying magnetic fields (Sec. IV B) in the LLL approximation. Here, $i = 1, 2, 3$ denotes the three spatial directions. As it turns out, in the regime of LLL dominance the electric susceptibility in the perpendicular direction relative to the external magnetic field (i.e. for $i = 1, 2$) vanishes in both homogeneous and inhomogeneous magnetic fields. The longitudinal component of $\chi^{(i)}$, denoted by $\chi^{\|}$, turns out to be constant in a homogeneous magnetic field and depend nontrivially on the dimensionless variable u in an exponentially decaying magnetic field. In Sec. V, we will compare the results for the chiral condensate and the local electric current correlation function arising from homogeneous and inhomogeneous magnetic fields and show that the limits $\xi \to 0$ as well as $x \to 0$ are singular. In other words, although in the limits $\xi \to 0$ and/or $x \to 0$, we get $B(x) \to B_0$, but the values of $\langle\bar{\psi}\psi\rangle$ and $\chi^{\|}$ arising from an exponentially decaying magnetic field in these limits are not the same as $\langle\bar{\psi}\psi\rangle$ and $\chi^{\|}$ arising from a homogeneous magnetic field. This demonstrates the nonlocal features of the quantum vacuum in a strong and spatially decaying magnetic field. As is indicated in Sec. VI, which is devoted to our concluding remarks, the results of this paper are relevant for high energy physics as well as condensed matter physics.

II. ELECTRONS IN EXTERNAL MAGNETIC FIELDS

Ritus eigenfunction method [15] is a powerful tool to study the dynamics of electrons in external electromagnetic fields. It is recently used in [16] to solve the Dirac equation in the presence of a uniform magnetic field in 2+1 dimensions, a uniform electric field in 1+1 dimensions and an exponentially decaying magnetic field in $2+1$ dimensions (see also [13]). In [17, 18], the Ritus method is used to solve the 3+1 dimensional Dirac equation for massless fermions in the presence of a constant magnetic field. In Sec. II A, we will briefly review the results from [18] and will present the solution of the Dirac equation for a single massive electron in the presence of a constant magnetic field in $3+1$ dimensions. This will fix our notations. In Sec. II B, we will use the same method and will solve the Dirac equation for a massive electron in an exponentially decaying magnetic field. Our results coincide with the result presented in [13], although our notations are slightly different. We will also present the final form of the fermion propagator in the presence of a uniform and an exponentially decaying magnetic field in Secs. II A and II B, respectively. The results presented in this section will then be used in Sec. III to determine the chiral condensate, and in Sec. IV the local electric current correlation function in the presence of uniform and non-uniform magnetic fields.

A. Electrons in constant magnetic fields

Let us start with the Dirac equation of a single electron in $3+1$ dimensional Minkowski space in a background electromagnetic field

$$(\gamma\cdot\Pi - m)\,\psi = 0, \qquad \text{(II.1)}$$

where $\Pi_\mu \equiv i\partial_\mu - eA_\mu$ and A_μ is the electromagnetic potential. Here, m and e are the electron's mass and electric charge, respectively. The aim is to solve (II.1) and to eventually determine the fermion propagator in the presence of background constant magnetic field $\mathbf{B} = B_0\mathbf{e}_z$, aligned in the third direction. Such a constant magnetic field, is built, for instance, by choosing the gauge field A_μ in the Landau gauge as $A_\mu = (0, 0, B_0 x, 0)$. To solve (II.1), we use, as in [16, 17], the Ansatz $\psi = \mathbb{E}_p u_{\tilde{p}}$. Here, $\mathbb{E}_p$ is a diagonal matrix satisfying

$$(\gamma\cdot\Pi)\ \mathbb{E}_p = \mathbb{E}_p\ (\gamma\cdot\tilde{p}), \tag{II.2}$$

and $u_{\tilde{p}}$ is a free spinor, that describes an electron with momentum $\tilde{p}$ and satisfies $(\gamma\cdot\tilde{p}-m)u_{\tilde{p}}=0$. The Ritus eigenfunction $\mathbb{E}_p$ and the Ritus momentum $\tilde{p}$ in (II.2) are unknown and shall be determined in what follows. The matrix $\mathbb{E}_p$ is determined by solving the eigenvalue equation

$$(\gamma\cdot\Pi)^2\ \mathbb{E}_p = \tilde{p}^2\mathbb{E}_p, \tag{II.3}$$

that arises directly from (II.2). Using $(\gamma\cdot\Pi)^2 = \Pi^2 + \frac{e}{2}\sigma^{\mu\nu}F_{\mu\nu}$, with $\sigma^{\mu\nu}\equiv\frac{i}{2}[\gamma^\mu,\gamma^\nu]$ and the field strength tensor $F_{\mu\nu}\equiv\partial_\mu A_\nu-\partial_\nu A_\mu$, with non-vanishing elements $F_{12}=-F_{21}=B_0$, and choosing, without loss of generality, the Dirac γ-matrices as $\gamma^0=\sigma_3\otimes\sigma_3$, and $\gamma^i = i\sigma_3\otimes\sigma_i$, where $\sigma_i, i=1,2,3$ are the Pauli matrices, (II.3) reads

$$\left(\Pi^2+\sigma^{12}eB_0\right)\mathbb{E}_p = \tilde{p}^2\mathbb{E}_p. \tag{II.4}$$

Here, $\sigma^{12}=i\gamma^1\gamma^2=\mathbb{I}\otimes\sigma_3$ with $\mathbb{I}$ a 2×2 identity matrix. To solve (II.4), we use the fact that in the Landau gauge, the operator $(\gamma\cdot\Pi)$ commutes with Π_0, $\Pi_j, j=2,3$ and $\mathcal{P}\equiv-(\gamma\cdot\Pi)^2+\Pi_0^2-\Pi_3^2$, and therefore has simultaneous eigenfunctions with these operators. The eigenvalues of these operators, defined by the eigenvalue equations

$$\begin{aligned}\Pi_0\mathbb{E}_p &= p_0\mathbb{E}_p, \qquad \Pi_j\mathbb{E}_p = p_j\mathbb{E}_p,\ j=2,3, \qquad \text{and}\\ \mathcal{P}\mathbb{E}_p &= p\ \mathbb{E}_p,\end{aligned} \tag{II.5}$$

label the solutions of Dirac equation (II.1) in the background magnetic field. Using (II.3), the definition of $\mathcal{P}$ and (II.5), it can be shown that the four-momentum $\tilde{p}$ satisfies $\tilde{p}^2=p_0^2-p_3^2-p$, and $\mathcal{P}\mathbb{E}_p=p\ \mathbb{E}_p$ is therefore given by

$$\left(\partial_x^2-(p_2-eB_0x)^2+\sigma^{12}eB_0\right)\mathbb{E}_p = -p\ \mathbb{E}_p. \tag{II.6}$$

Before solving (II.6), let us determine the components of Ritus momentum $\tilde{p}$, which turns out to play an important role in this method. To do this, we consider (II.2), and use the Ansatz

$$\mathbb{E}_p = \sum_{\sigma=\pm}\Delta_\sigma E_{p,\sigma}, \tag{II.7}$$

with the projectors [17]

$$\Delta_\sigma\ \equiv\ \text{diag}\left(\delta_{\sigma,1},\delta_{\sigma,-1},\delta_{\sigma,1},\delta_{\sigma,-1}\right). \tag{II.8}$$

Plugging first $\mathbb{E}_p$ from (II.7) in the left hand side (l.h.s) of (II.2), and then comparing the resulting expression with the expression arising from the right hand side (r.h.s.) of (II.2), where again $\mathbb{E}_p$ from (II.7) and the Ansatz $\tilde{p}=(p_0,0,\tilde{p}_2,p_3)$ is used,[1] we arrive at (II.6), with p given by $p=\tilde{p}_2^2$. This will fix $\tilde{p}_2=-\sqrt{p}$.[2]

Let us now turn back to the solution of (II.6), whose form suggests a plane wave Ansatz in the $0,2$ and 3 directions,

$$E_{p,\pm1}(\bar{x}) = e^{-i\bar{p}\cdot\bar{x}}f_p^\pm(x), \tag{II.9}$$

where $\bar{x}=(t,x,y,z)$ and $\bar{p}=(p_0,0,p_2,p_3)$. Plugging (II.9) in (II.7), and using $\Delta_\pm=\frac{1}{2}\left(1\pm i\gamma^1\gamma^2\right)$ for the projectors defined in (II.8), the general solution for $\mathbb{E}_p$ is given by

$$\mathbb{E}_p(\bar{x}) = e^{-i(p_0t-p_2y-p_3z)}P_p(x), \tag{II.10}$$

where

$$P_p(x) = \frac{1}{2}\{[f_p^+(x)+f_p^-(x)]+i\gamma^1\gamma^2[f_p^+(x)-f_p^-(x)]\}. \tag{II.11}$$

To determine $f_p^\pm(x)$, it is enough to replace $\mathbb{E}_p(\bar{x})$ from (II.10) in (II.6) to arrive at

$$\left(\partial_x^2-(p_2-eB_0x)^2\pm eB_0\right)f_p^\pm(x) = -pf_p^\pm(x). \tag{II.12}$$

Renaming the discrete quantum numbers $\sqrt{p}$ in the four-momentum $\tilde{p}$ by $\sqrt{p}=\text{sgn}(eB_0)\sqrt{2|eB_0|p}$, and choosing a new coordinate $\zeta\equiv\frac{\sqrt{2}}{\ell_B}(x-\ell_B^2p_2)$, with ℓ_B the magnetic length defined by $\ell_B\equiv|eB_0|^{-1/2}$, the differential equation in (II.12) can be reformulated in the form of the differential equation of harmonic oscillator, whose center lies in $\bar{x}_0=p_2/eB_0$ and oscillates with the cyclotron frequency $\omega_c=2eB_0$ [16],

$$\left(\frac{\partial^2}{\partial\zeta^2}+p+\frac{\sigma}{2}\text{sgn}(eB_0)-\frac{\zeta^2}{4}\right)f_p^\pm(\zeta)=0. \tag{II.13}$$

As it turns out, the solution to the above equation can be given in terms of parabolic cylinder function [16, 17]

$$\begin{aligned}\phi_{n_\sigma}(x) &= a_{n_\sigma}\exp\left(-\frac{x^2}{2\ell_B^2}\right)H_{n_\sigma}\left(\frac{x}{\ell_B}\right),\\ \text{with}\qquad a_{n_\sigma} &\equiv \frac{1}{\sqrt{2^{n_\sigma}n_\sigma!\ell_B\sqrt{\pi}}},\end{aligned} \tag{II.14}$$

where n_σ is, in general, given by

$$n_\sigma = p+\frac{\sigma}{2}\text{sgn}(eB_0)-\frac{1}{2}. \tag{II.15}$$

---

[1] The form $\tilde{p}^2=p_0^2-p_3^2-p$ suggests that $\tilde{p}_1=0$. Moreover, we have fixed $\tilde{p}_i=p_i, i=0,3$, where according to (II.5) $p_i, i=0,3$ are the eigenvalue of $\Pi_i, i=0,3$, respectively.

[2] Note that the general solution for $\tilde{p}_2$ is either $+\sqrt{p}$ or $-\sqrt{p}$. Here, we have chosen $\tilde{p}_2=-\sqrt{p}$ to have the same notation as in [18].

Here, p labels the energy (Landau) levels. In the rest of this paper, we will work with $eB_0 > 0$. According to (II.15), for $\text{sgn}(eB_0) > 0$, the condition that $n_\sigma \geq 0$ for $p = 0$, fixes the spin orientation of the electrons in the LLL to be positive ($\sigma = +1$). In this case n_+ will be given by $n_+ = p$ for all values of p [17]. For this specific choice, the final result for $f_p^\pm(x)$ is the same as the result presented in [18],

$$\begin{aligned} f_p^+(x) &= \phi_p\left(x - \ell_B^2 p_2\right), \qquad & p = 0,1,2,\cdots, \\ f_p^-(x) &= \phi_{p-1}\left(x - \ell_B^2 p_2\right), \qquad & p = 1,2,3,\cdots. \end{aligned} \tag{II.16}$$

Hence, for $eB_0 > 0$, only the positive spin solution $f_0^+(x)$ contributes in the LLL, characterized by $p = 0$. In other words, $f_0^-(x) = f_{-1}^+(x)$ is undefined and is to be neglected, whenever it appears in a computation.

The energy dispersion relation for an electron in the presence of a constant magnetic field is determined by the Ritus momentum

$$\tilde{p}_p = \left(p_0, 0, -\sqrt{2eB_0 p}, p_3\right), \tag{II.17}$$

and is given by

$$\mathcal{E}_p = \sqrt{2eB_0 p + p_3^2 + m^2}, \quad p = 0,1,2,\cdots. \tag{II.18}$$

The Ritus eigenfunction $\mathbb{E}_p$ from (II.10) can be used to determine the fermion propagator in the presence of a uniform magnetic field. To do this, the Ansatz $\psi = \mathbb{E}_p u_{\bar{p}}$ for the electron is to be generalized to a system including particles and antiparticles. Defining the associated creation and annihilation operators, and following the standard steps to determine the propagator [19], the fermion propagator in the presence of a constant magnetic field is given by (see also [18])

$$\begin{aligned} G(\bar{x}, \bar{x}') &\equiv \langle \psi(\bar{x}) \bar{\psi}(\bar{x}') \rangle \\ &= \sum_{p=0}^{\infty} \int \mathcal{D}\bar{p}\; e^{-i\bar{p}\cdot(\bar{x}-\bar{x}')} P_p(x) \frac{i}{(\gamma \cdot \tilde{p}_p - m)}\; P_p(x'), \end{aligned} \tag{II.19}$$

where $\mathcal{D}\bar{p} \equiv \frac{dp_0 dp_2 dp_3}{(2\pi)^3}$, $P_p(x)$ is given in (II.11) with $f_p^\pm(x)$ from (II.16), and the Ritus momentum $\tilde{p}_p$ is given in (II.18). The same expression appears also in [18]. Since we are working with $eB_0 > 0$, and the spin orientation of the electrons are already fixed in the LLL to be positive, no spin projector appears in (II.19), as in the fermion propagators presented in [17]. To understand this, let us notice again that the facts that LLL includes only the positive spin solution, and that negative spin solutions contribute only to the higher Landau levels, are explicitly implemented in the choice $p = 0,1,2,\cdots$ for positive spin solution $f_p^+(x)$, and $p = 1,2,3,\cdots$ for negative spin solution $f_p^-(x) = f_{p-1}^+(x)$ in (II.16). In Sec. II B, we will use the above method to determine the energy dispersion relation and the propagator for electrons in the presence of exponentially decaying magnetic fields.

B. Electrons in exponentially decaying magnetic fields

In this section, the Ritus eigenfunction method will be used to determine the energy levels of a single fermion in the presence of an exponentially decaying magnetic field $\mathbf{B}(x) = B_0 e^{-\alpha x}\hat{\mathbf{e}}_z$, aligned in the third direction. Here, B_0 is the magnetic field at $x = 0$, α is a dimensionful damping parameter. Later, we will set $\alpha = \xi\sqrt{eB_0}$, where ξ is a given dimensionless damping parameter and $eB_0 > 0$. The dynamics of this electron in such an inhomogeneous magnetic field is described by the Dirac equation (II.1). To solve it, we fix the gauge, in contrast to the previous case, by $A_\mu(x) = \left(0, 0, -\frac{B_0}{\alpha}(e^{-\alpha x} - 1), 0\right)$, as in [13]. With this choice of A_μ, the case of constant magnetic field will be recovered by taking the limit $\alpha \to 0$ (or equivalently $\xi \to 0$) in the classical level. Using the Ansatz $\psi = \mathbb{E}_{\bar{p}} u_{\bar{p}}$, with $\mathbb{E}_p$ satisfying (II.2), and following the same steps leading from (II.2) to (II.6), we arrive at

$$\begin{aligned} &\left[\partial_x^2 - \left(i\partial_y - \frac{eB_0}{\alpha}(e^{-\alpha x} - 1)\right)^2 + \sigma eB_0 e^{-\alpha x}\right]\mathbb{E}_p \\ &\qquad = -p\; \mathbb{E}_p, \end{aligned} \tag{II.20}$$

where $\sigma = \pm 1$ are the eigenvalues of third Pauli matrix, $\sigma_3 = \text{diag}(1, -1)$. Using in analogy to (II.7), a plane wave Ansatz for $\mathbb{E}_p$,[3]

$$\mathbb{E}_p(\rho) = \sum_{\sigma=\pm} \Delta_\sigma E_{p,\sigma}(\rho), \tag{II.21}$$

with Δ_σ defined in (II.8), and $E_{p,\sigma}(\rho) = e^{i\bar{p}\cdot\bar{x}} F_{n_\sigma}^k(u)$, we arrive first at

$$\begin{aligned} &\left[u^2 \frac{\partial^2}{\partial u^2} + u\frac{\partial}{\partial u} - \frac{u^2}{4}\right. \\ &\qquad \left. + \left(\frac{\hat{p}_2}{\alpha} + \frac{\sigma}{2}\right)u + \frac{(p - \hat{p}_2^2)}{\alpha^2}\right] F_{n_\sigma}^k(u) = 0. \end{aligned} \tag{II.22}$$

In the above equations, $\rho \equiv (t, u, y, z)$ where u is a dimensionless variable defined by $u \equiv \frac{2}{\alpha^2} eB_0 e^{-\alpha x}$. Moreover, $\hat{p}_2 = p_2 + eB_0/\alpha$, and $(\bar{x}, \bar{p})$ are given as in the previous section [see below (II.9)]. Comparing (II.22) with the differential equation

---

[3] Note that the plane wave Ansatz is justified by $[\mathcal{P}, i\partial_3] = [\mathcal{P}, i\partial_0] = 0$, where $\mathcal{P}$ is defined by $\mathcal{P} = -(\gamma\cdot\Pi)^2 + \Pi_0^2 - \Pi_3^2$, as in Sec. II A.

$$\left[u^2\frac{\partial^2}{\partial u^2}+u\frac{\partial}{\partial u}-\frac{u^2}{4}\right.$$
$$\left.+\frac{(2n+k+1)}{2}u-\frac{k^2}{4}\right]\Phi_n^k(u)=0, \quad \text{(II.23)}$$

satisfied by

$$\Phi_n^k(u)=\sqrt{\frac{n!}{(n+k)!}}e^{-u/2}e^{k/2}\mathcal{L}_n^k(u), \quad \text{(II.24)}$$

where $\mathcal{L}_n^k(u)$ is the associated Laguerre polynomial, the quantum numbers k and n_σ are given by

$$\begin{aligned} k &= \frac{2}{\alpha}\sqrt{\hat{p}_2^2-p}, \qquad \text{and} \\ n_\sigma &= \frac{\sigma}{2}-\frac{1}{2}+\frac{\hat{p}_2-\sqrt{\hat{p}_2^2-p}}{\alpha}. \end{aligned} \quad \text{(II.25)}$$

Note that the indices k and n_σ in $\mathcal{L}_{n_\sigma}^k$ are to be positive integers. This implies the following quantization for $\hat{p}_2$ and p

$$\lfloor\frac{\hat{p}_2}{\alpha}\rfloor\equiv s, \qquad \text{and} \qquad p\equiv\alpha^2(s^2-r^2), \quad \text{(II.26)}$$

leading to $k=2r$, with $r>0$, and

$$n_\sigma=\frac{\sigma}{2}-\frac{1}{2}+s-r. \quad \text{(II.27)}$$

In (II.26), $\lfloor a\rfloor$ is the greatest integer less than or equal to a. As it is shown in [11–13], $s=\lfloor p_2/\alpha\rfloor$ is associated with certain constant length $\ell_0\equiv\frac{e^{\alpha x_0}}{\sqrt{eB_0}}$, through the relation

$$s=\lfloor\frac{\hat{p}_2}{\alpha}\rfloor=\lfloor\frac{1}{(\alpha\ell_0)^2}\rfloor, \quad \text{(II.28)}$$

where x_0 is a fixed length. At this stage, let us compare, n_σ from (II.27) with n_σ appearing in (II.15) for $eB_0>0$.[4] As it turns out, in the case of exponentially decaying magnetic field, $s-r$ labels the energy levels. In analogy to the case of constant magnetic field, to keep n_σ from (II.27) positive, the electron spin orientation σ in the lowest energy level, characterized by $s-r=0$, is fixed to be positive ($\sigma=+1$). In this case, we have $n\equiv n_+=s-r$. What concerns the quantum numbers r and s, for $r>0$, we get $s\geq r$, that guarantees $n=s-r\geq 0$. In analogy to the solutions (II.16), for the constant magnetic fields, we arrive therefore at

$$F_n^{2r}(u)\equiv F_{n_+}^{2r}(u)=N_{n,r}e^{-\frac{u}{2}}u^r\mathcal{L}_n^{2r}(u), \quad \text{(II.29)}$$

with $n=s-r=0,1,2,\cdots$, for positive spin solutions and

$$F_{n-1}^{2r}(u)\equiv F_{n_-}^{2r}(u)=N_{n-1,r}e^{-\frac{u}{2}}u^r\mathcal{L}_{n-1}^{2r}(u), \quad \text{(II.30)}$$

with $n=s-r=1,2,3,\cdots$, for negative spin solutions. Using the orthonormality relations of associated Legendre polynomials $\mathcal{L}_n^{2r}$, the normalization factor $N_{n,r}$ is given by

$$N_{n,r}\equiv\sqrt{\frac{n!}{(n+2r)!}}.$$

Using finally the projection matrices $\Delta_\pm=\frac{1}{2}(1\pm i\gamma^1\gamma^2)$, the solution for $\mathbb{E}_n$ can be brought in the form similar to the Ritus eigenfunction (II.10) and (II.11) for constant magnetic field,

$$\mathbb{E}_p(\rho)=e^{-i(p_0t-p_2y-p_3z)}P_n^{2r}(u), \quad \text{(II.31)}$$

with

$$P_n^{2r}(u)=$$
$$\frac{1}{2}\big\{[F_n^{2r}(u)+F_{n-1}^{2r}(u)]+i\gamma^1\gamma^2[F_n^{2r}(u)-F_{n-1}^{2r}(u)]\big\}. \quad \text{(II.32)}$$

Using the orthonormality conditions for the associated Laguerre polynomials, $\mathcal{L}_n^{2r}(u)$, presented in App. A, it is straightforward to derive the closure and the orthonormality relations for $\mathbb{E}_p$,

$$\alpha\sum_{r=1}^{\infty}\sum_{s=r}^{\infty}\int\frac{d^2\mathbf{p}_\parallel}{(2\pi)^2}\ \mathbb{E}_p(\rho)\bar{\mathbb{E}}_p(\rho')=\hat{\delta}(\rho-\rho'), \quad \text{(II.33)}$$

as well as

$$\int\mathcal{D}\rho\ \mathbb{E}_p(\rho)\bar{\mathbb{E}}_{p'}(\rho)=\alpha^{-1}\delta^2(\mathbf{p}_\parallel-\mathbf{p}'_\parallel)\delta_{s,s'}\Pi^s_{r,r'}. \quad \text{(II.34)}$$

In the above relations, $\alpha\equiv\xi\sqrt{eB_0}$, $\bar{\mathbb{E}}_p(\rho)\equiv\gamma_0\mathbb{E}_p^\dagger(\rho)\gamma_0$, $\mathbf{p}_\parallel\equiv(p_0,p_3)$ and $\hat{\delta}(\rho-\rho')\equiv\delta(t-t')\delta(u-u')\delta(y-y')\delta(z-z')$, $\mathcal{D}\rho\equiv dtdudydz$, and

$$\Pi^s_{r,r'}=\Delta_+\delta_{r,r'}\delta_{s,r}+(1-\delta_{s,r})\Bigg[\delta_{r,r'}$$
$$+\Bigg\{\theta(r'-r)(-1)^{r'-r}\sqrt{\frac{\Gamma(s+r)\Gamma(s-r)}{\Gamma(s+r')\Gamma(s-r')}}$$
$$\times\left(\Delta_+\sqrt{\frac{(s^2-r^2)}{(s^2-r'^2)}}+\Delta_-\right)+r\to r'\Bigg\}\Bigg], \quad \text{(II.35)}$$

with $\Delta_\pm$ given in (II.8). These relations are similar to the results presented in [13]. Note that the term proportional to $\delta_{r,s}$ isolates the contribution of the lowest energy level, characterized by $s=r$. This term is also proportional to Δ_+, implying that the spin orientation in the lowest energy level for $eB_0 > 0$ is positive. What concerns the contribution of higher energy levels, we had to distinguish between $r = r'$, $r > r'$ and $r < r'$ cases. This is because plugging $\mathbb{E}_p$ from (II.31) and (II.32) in the l.h.s. of (II.34), leads in general to the orthonormality relations similar to (A.1) in App. A, where r and r' are not necessarily equal. In App. A, the orthonormality relation (A.1) is determined separately for $r = r'$, $r > r'$ and $r < r'$. Using these results, it is straightforward to derive the remaining terms in (II.35), arising from higher energy levels.

---

[4] Comparing to (II.15), n_σ from (II.27), is in general given by $n_\sigma=\frac{\sigma}{2}\text{sgn}(eB_0)-\frac{1}{2}+s-r$.

To determine the Ritus momentum $\tilde{p}$, we insert the above solution (II.31) and (II.32) for $\mathbb{E}_p$ in (II.2). After some straightforward algebraic manipulations, where we use the recursion relations of the Laguerre polynomials $\mathcal{L}_n^{2r}(u)$, we arrive at

$$(\gamma\cdot\Pi)\mathbb{E}_p = \mathbb{E}_p[\gamma^0 p_0 + \gamma^2\alpha\sqrt{n(n+2r)} - \gamma^3 p_3]. \quad \text{(II.36)}$$

Here, $n = s - r$ and $\alpha = \xi\sqrt{eB_0}$. Comparing the r.h.s. of (II.36) with (II.2), we get $\tilde{p} = \left(p_0, 0, -\alpha\sqrt{n\,(n+2r)}, p_3\right)$, which can alternatively be given in terms of (s, r) and ξ as

$$\tilde{p}_\kappa = \left(p_0, 0, -\xi\sqrt{eB_0\kappa}, p_3\right), \quad \text{(II.37)}$$

with $\kappa \equiv s^2 - r^2$. Using (II.37), the energy dispersion relation of a single electron in an exponentially decaying magnetic field is given by

$$\mathcal{E}_\kappa = \sqrt{\xi^2 eB_0\kappa + p_3^2 + m^2}, \quad \text{(II.38)}$$

which is to be compared with the energy dispersion relation of an electron in the presence of a constant magnetic field from (II.18). Let us notice, that although $n = s - r$ labels the energy levels, in contrast to the case of constant magnetic field, $\kappa = s^2 - r^2$ determines the ordering of energy levels. Because of the above mentioned conditions for the integer quantum numbers $r > 0$, $s \geq r$ (or $n \geq 0$), some value of κ are not allowed. The simplest way to determine κ, is to write it in terms of n and r as $\kappa = n(n+2r)$. Choosing $r = 1, 2, \cdots$, then κ turns out to be $\kappa = 0$ for $n = 0$ (or all values of $r = s$), $\kappa = 3, 5, 7, \cdots, 1+2r$ for $n = 1$, $\kappa = 8, 12, 16, \cdots, 2(2+2r)$ for $n = 2$, etc. In Secs. III and IV, the summation over energy levels in an exponentially decaying magnetic field will be replaced by $\sum_{r=1}^{\infty}\sum_{s=r}^{\infty} g(r, s)$. Here, $g(r, s)$ is a generic function, that depends on the quantum numbers r and s. According to the above descriptions, the lowest energy level is then characterized by $\sum_{r=1}^{\infty} g(r, s = r)$, or equivalently by $\sum_{r=1}^{\infty} g(r, n = 0)$.

Following the description presented at the end of the previous section, the fermion propagator of an electron in an exponentially decaying magnetic field is given by (see also [13])

$$\begin{aligned} G(\rho, \rho') &\equiv \langle\psi(\rho)\bar{\psi}(\rho')\rangle \\ &= \alpha^2\sum_{r=1}^{\infty}\sum_{s=r}^{\infty}\int\frac{d^2\mathbf{p}_\parallel}{(2\pi)^2}\,\mathbb{E}_p(\rho)\frac{i}{(\gamma\cdot\tilde{p}_\kappa - m)}\bar{\mathbb{E}}_p(\rho'), \end{aligned} \quad \text{(II.39)}$$

where $\mathbb{E}_p(\rho)$ and $\tilde{p}_\kappa$ are given in (II.31)-(II.32) and (II.37), respectively. Using (II.2) and the closure of $\mathbb{E}_p(\rho)$ from (II.33), it is easy to verify

$$(\gamma\cdot\Pi - m)\,G(\rho - \rho') = \delta^4(\rho - \rho'), \quad \text{(II.40)}$$

where $\delta^4(\rho - \rho') \equiv \alpha\delta(t - t')\delta(u - u')\delta(y - y')\delta(z - z')$. Here, as in the case of constant magnetic fields, since we are working with $eB_0 > 0$, the spin orientation in the lowest energy level is fixed to be positive, and the negative spin electrons contribute only to higher energy levels. These facts are explicitly implemented in the choice $n = s - r = 0, 1, 2, \cdots$ for positive spin solution $F_n^{2r}(u)$ and $n = s - r = 1, 2, 3, \cdots$ for negative spin solution $F_{n-1}^{2r}(x)$ in (II.29) and (II.30), respectively.[5]

III. FERMION CONDENSATE $\langle\bar{\psi}\psi\rangle$ IN EXTERNAL MAGNETIC FIELDS

In this section, we will determine the fermion condensate $\langle\bar{\psi}\psi\rangle$ in the presence of constant and exponentially decaying magnetic fields. The fermion condensate is defined by [20]

$$\langle\bar{\psi}\psi\rangle = -\lim_{x\to x'}\mathrm{tr}[G_F(x - x')], \quad \text{(III.1)}$$

where $G_F(x - x')$ is the fermion propagator in the presence of an external magnetic field, in general. In [5], Schwinger's proper-time formalism is used to determine $\langle\bar{\psi}\psi\rangle$ in a constant magnetic field in the LLL approximation. In this section, we will use the Ritus method, and in particular, our results from the previous section to determine $\langle\bar{\psi}\psi\rangle$ first in a constant and then in an exponentially decaying magnetic field, in the LLL approximation, at finite temperature and chemical potential.

A. $\langle\bar{\psi}\psi\rangle$ in constant magnetic fields

To determine the fermion condensate in a constant magnetic field, let us replace $G(\bar{x} - \bar{x}')$ from (II.19) in (III.1). Performing the traces over γ-matrices, we arrive at

---

[5] In other words, $F_{-1}^{2r}(u)$ is undefined and is to be neglected, whenever it appears in a computation.

$$\langle\bar{\psi}\psi\rangle^{c} = -2im\sum_{p=0}^{\infty}\int\frac{dp_0dp_2dp_3}{(2\pi)^3}\frac{1}{(p_0^2-\omega_p^2)}\times\{[f_p^{+}(x)]^2+[f_{p-1}^{+}(x)]^2\}, \tag{III.2}$$

where according to (II.17), the ω_p for $eB_0>0$ is defined by $\omega_p^2\equiv 2eB_0p+p_3^2+m^2$. In the LLL approximation, we shall set $p=0$. Using the definition of $f_p^{+}(x)$ from (II.16), and after performing the integration over p_2,

$$\int\frac{dp_2}{2\pi}[f_0^{+}(x)]^2=\frac{eB_0}{2\pi}, \tag{III.3}$$

we arrive at

$$\langle\bar{\psi}\psi\rangle^{c}_{\text{LLL}}=-\frac{imeB_0}{\pi}\int\frac{dp_0dp_3}{(2\pi)^2}\,\frac{1}{(p_0^2-\omega_0^2)}, \tag{III.4}$$

where $\omega_0^2\equiv p_3^2+m^2$. The dimensional reduction into two longitudinal dimensions $\mathbf{p}_{\parallel}=(p_0,p_3)$, which occurs whenever the LLL approximation is used [5], can be observed in (III.4). To evaluate (III.4), we use

$$\int\frac{d^2\mathbf{p}_{\parallel}}{(2\pi)^2}\,\frac{1}{(\mathbf{p}_{\parallel}^2-m^2)}\overset{\Lambda\gg m}{\longrightarrow}\frac{i}{4\pi}\ln\left(\frac{m^2}{\Lambda^2}\right), \tag{III.5}$$

which yields the fermion condensate in the presence of a constant magnetic field in the lowest Landau level,

$$\langle\bar{\psi}\psi\rangle^{c}_{\text{LLL}}=\frac{meB_0}{4\pi^2}\ln\left(\frac{m^2}{\Lambda^2}\right)+\mathcal{O}(m). \tag{III.6}$$

Here, Λ is an appropriate momentum cutoff. This result coincides exactly with the result presented in [5], where the method of proper-time is used. Note that although no integration over the coordinates $\bar{x}=(t,x,y,z)$ is performed here, the condensate (III.6) is constant in $\bar{x}$. This is mainly because of the special form of $f_0^{+}(x)$ from (II.16) and arises from the integration over p_2 in (III.3). In Sec. III B, we will show that in the presence of an exponentially decaying magnetic field, the condensate $\langle\bar{\psi}\psi\rangle$ in the LLL depends nontrivially on x. Let us also notice that in massless QED, the mechanism of magnetic catalysis [4, 5] is made responsible for dynamically breaking of chiral symmetry and the generation of a finite dynamical mass in the LLL. Moreover, as it is shown in [21], apart from a dynamical mass induced by the external magnetic field in the LLL, an anomalous magnetic moment is also induced, so that the dynamical mass in the LLL is to be replaced by the rest energy E_0, which is a combination of the induced dynamical mass and the anomalous magnetic moment in the LLL. In this paper, we do not consider the effects of dynamically induced anomalous magnetic moment on the dynamically generated fermion mass. The latter arises either as a solution of an appropriate Schwinger-Dyson equation in a ladder approximation or by solving a corresponding gap equation to an appropriate effective potential in the mean field approximation. In what follows, we will compute $\langle\bar{\psi}\psi\rangle^{c}_{\text{LLL}}$ from (III.6) at finite temperature T and finite density μ. To do this we use the standard imaginary time formalism, and replace p_0 in (III.4) by $ip_4=i(\omega_\ell+i\mu)$, where $\omega_\ell=\pi(2\ell+1)T$ is the Matsubara frequency labeled by ℓ. Thus the integration over p_0 is to be replaced by

$$\int\frac{dp_4}{2\pi}\to\frac{1}{\beta}\sum_{\ell=-\infty}^{\infty}, \tag{III.7}$$

where $\beta^{-1}\equiv T$. The fermion condensate $\langle\bar{\psi}\psi\rangle^{c}_{\text{LLL}}$ at finite T and μ is therefore given by

$$\langle\bar{\psi}\psi\rangle^{c}_{\text{LLL}}=-\frac{meB_0}{\pi\beta}\sum_{\ell=-\infty}^{\infty}\int\frac{dp_3}{2\pi}\frac{1}{(p_4^2+p_3^2+m^2)}. \tag{III.8}$$

To evaluate the integration over p_3 and the summation over ℓ, the relation

$$\frac{1}{\beta}\sum_{\ell=-\infty}^{\infty}\int\frac{d^dp}{(2\pi)^d}\frac{(\mathbf{p}^2)^a p_4^{2t}}{(p_4^2+\mathbf{p}^2+m^2)^\sigma}=\frac{1}{2(4\pi)^{d/2}\Gamma(\sigma)\beta}\frac{\Gamma\left(\frac{d}{2}+a\right)}{\Gamma\left(\frac{d}{2}\right)}\left(\frac{2\pi}{\beta}\right)^{-2\sigma+d+2(t+a)}\times\sum_{k=0}^{\infty}\frac{(-1)^k}{k!}\Gamma\left(\sigma-a+k-\frac{d}{2}\right)\left[\zeta\left(2\left(\sigma+k-t-a\right)-d;\frac{1}{2}-\frac{i\beta\mu}{2\pi}\right)+(\mu\to-\mu)\right]\left(\frac{m\beta}{2\pi}\right)^{2k}, \tag{III.9}$$

from [22] will be used. This relation (III.9) is originally derived in [23] for $\mu=0$. In (III.9), $\zeta\left(s;a\right)$ is the Hurwitz zeta function defined by $\zeta(s;a)=\sum_{k=0}^{\infty}(k+a)^{-s}$, where any term with $k+a=0$ is excluded. In an evaluation up to $\mathcal{O}((m\beta)^4)$, we get finally

$$
\begin{aligned}
\langle\bar{\psi}\psi\rangle_{\rm LLL}^{c} = &-\frac{meB_0}{8\pi^2}\bigg\{2\ln\left(\frac{m\beta}{2\pi}\right)-\gamma_E\\
&-\left[\psi\left(\frac{1}{2}+\frac{i\beta\mu}{2\pi}\right)+\psi\left(\frac{1}{2}-\frac{i\beta\mu}{2\pi}\right)\right]\\
&-\frac{(m\beta)^2}{8\pi^2}\left[\zeta\left(3;\frac{1}{2}+\frac{i\beta\mu}{2\pi}\right)+\zeta\left(3;\frac{1}{2}-\frac{i\beta\mu}{2\pi}\right)\right]\bigg\}\\
&+\mathcal{O}((m\beta)^4), \qquad \text{(III.10)}
\end{aligned}
$$

where $\gamma_E \sim 0.557$ is the Euler-Mascheroni number and $\psi(z)$ the polygamma function, defined by $\psi(z) = \frac{d}{dz}\ln\Gamma(z)$. It arises by an appropriate regularization of $\zeta(1;a)$ using

$$
\lim_{\epsilon\to 0}\zeta(1+\epsilon;a) = \lim_{\epsilon\to 0}\frac{1}{\epsilon}-\psi(a). \qquad \text{(III.11)}
$$

In (III.10), the divergent $1/\epsilon$ term is neglected, and the identity $\psi(1/2) = -\gamma_E - 2\ln 2$ is used.

B. $\langle\bar{\psi}\psi\rangle$ in exponentially decaying magnetic fields

The chiral condensate in an exponentially decaying magnetic field is given by (III.1), where $S_F(x-x')$ is to be replaced by $G(\rho-\rho')$ from (II.39). Performing the trace of Dirac matrices, we get first

$$
\begin{aligned}
\langle\bar{\psi}\psi\rangle &= -2i\xi^2 meB_0\sum_{r=1}^{\infty}\sum_{s=r}^{\infty}\int\frac{dp_0dp_3}{(2\pi)^2}\,\frac{1}{(p_0^2-\omega_\kappa^2)}\\
&\quad\times\{[F_n^{2r}(u)]^2+[F_{n-1}^{2r}(u)]^2\}, \qquad \text{(III.12)}
\end{aligned}
$$

where, according to (II.37), $\omega_\kappa^2 \equiv \xi^2 eB_0\kappa + p_3^2 + m^2$ and $\kappa = s^2 - r^2$. The expression on the r.h.s. of (III.12) includes the contributions of all energy levels, denoted by r and s, and the terms proportional to $(F_n^{2r})^2$ and $(F_{n-1}^{2r})^2$ correspond to the contributions of electrons with positive and negative spins, respectively. In the presence of strong magnetic fields, assuming that the dynamics of the system is solely determined by the LLL, the fermion condensate is given by

$$
\begin{aligned}
\langle\bar{\psi}\psi\rangle_{\rm LLL} &= -2i\xi^2 meB_0 e^{-u}[\cosh(u)-1]\\
&\quad\times\int\frac{dp_0dp_3}{(2\pi)^2}\frac{1}{(p_0^2-\omega_0^2)}, \qquad \text{(III.13)}
\end{aligned}
$$

in contrast to (III.4). The u-dependent factor behind the integral arises by setting $n = 0$ in (III.12) and using $\mathcal{L}_0^{2r} = 1$ and

$$
\sum_{r=1}^{\infty}[F_0^{2r}(u)]^2 = e^{-u}\sum_{r=1}^{\infty}\frac{u^{2r}}{(2r)!} = e^{-u}\left(\cosh u - 1\right).
$$

Note that in (III.13), the same dimensional reduction to two dimensions, as in the case of constant magnetic field, occurs. Evaluating the $\mathbf{p}_{\|}$-integration using (III.5), we get

$$
\begin{aligned}
\langle\bar{\psi}\psi\rangle_{\rm LLL} &= \frac{\xi^2 meB_0}{2\pi}e^{-u}\left(\cosh u-1\right)\ln\left(\frac{m^2}{\Lambda^2}\right)\\
&\quad+\mathcal{O}(m). \qquad \text{(III.14)}
\end{aligned}
$$

In contrast to (III.6), the fermion condensate in an exponentially decaying magnetic field, (III.14), depends on $u = \frac{2}{\xi^2}e^{-\xi\eta}$ with $\eta \equiv x/\ell_B$, and $\ell_B = (eB_0)^{-1/2}$, the magnetic length corresponding to B_0, the value of the magnetic field at $x = 0$. Following the same method to introduce finite temperature and chemical potential as in the Sec. III A, we arrive at

$$
\begin{aligned}
\langle\bar{\psi}\psi\rangle_{\rm LLL} = &-\frac{\xi^2 meB_0}{4\pi}\,e^{-u}(\cosh(u)-1)\bigg\{2\ln\left(\frac{m\beta}{2\pi}\right)\\
&-\gamma_E-\left[\psi\left(\frac{1}{2}+\frac{i\beta\mu}{2\pi}\right)+\psi\left(\frac{1}{2}-\frac{i\beta\mu}{2\pi}\right)\right]\\
&-\frac{(m\beta)^2}{8\pi^2}\left[\zeta\left(3;\frac{1}{2}+\frac{i\beta\mu}{2\pi}\right)+\zeta\left(3;\frac{1}{2}-\frac{i\beta\mu}{2\pi}\right)\right]\bigg\}\\
&+\mathcal{O}((m\beta)^4). \qquad \text{(III.15)}
\end{aligned}
$$

In Sec. V, we will compare the chiral condensates (III.6) and (III.14), as well as (III.10) and (III.15), arising from constant and exponentially decaying magnetic fields, respectively.

IV. LOCAL ELECTRIC CURRENT CORRELATION FUNCTION IN EXTERNAL MAGNETIC FIELDS

In this section, we will determine the *local* electric current correlation function $\chi^{(i)}(x)$ in homogeneous and inhomogeneous magnetic fields. It is defined generically by

$$
\chi^{(i)}(x) \equiv \lim_{x'\to x}\sum_n \chi_n^{(i)}(x,x'), \qquad \text{(IV.1)}
$$

with

$$
\begin{aligned}
&\chi_n^{(i)}(x,x')\\
&\quad\equiv\int\mathcal{D}\hat{x}\mathcal{D}\hat{x}'\,{\rm tr}\big[\gamma^i G_F^{(n)}(\bar{x},\bar{x}')\gamma^i G_F^{(n)}(\bar{x}',\bar{x})\big], \qquad \text{(IV.2)}
\end{aligned}
$$

where $i = 1,2,3$ are the spatial dimensions, and the sub- and superscripts n on $\chi_n^{(i)}$ and $G_F^{(n)}$ indicate the contribution of each energy (Landau) level to the local electric current correlation function $\chi^{(i)}(x)$ and the fermion propagator G_F, respectively. Moreover, $\mathcal{D}\hat{x} \equiv dtdydz$ and $\bar{x} = (t,x,y,z)$. Up to an integration over x,[6] the above definition is consistent with the definition of electric current susceptibility $\chi^{(i)}$ presented in [18]. In what follows, we will replace $G_F(\bar{x}-\bar{x}')$ in (IV.2) by (II.19) and (II.39) to determine the local electric current correlation function in constant and exponentially decaying magnetic fields, respectively.

A. $\chi^{(i)}(x)$ in constant magnetic fields

For a constant magnetic field, the contribution of $\chi_p^{(i)}(x,x')$ corresponding to each Landau level, labeled by p, is given by

$$\chi_p^{(i)}(x,x') = \int \mathcal{D}\hat{x}\mathcal{D}\hat{x}'\text{tr}\big[\gamma^i G_p(x,x')\gamma^i G_p(x',x)\big], \tag{IV.3}$$

where $\mathcal{D}\hat{x} = dtdydz$. Using (II.19) and plugging

$$G_p(x,x') = \int \mathcal{D}\bar{p}\; e^{i\bar{p}\cdot(\bar{x}-\bar{x}')}P_p(x)\frac{i}{\gamma\cdot\tilde{p}_p - m}P_p(x'), \tag{IV.4}$$

with $P_p(x)$ from (II.11) and $\tilde{p}_p$ from (II.17) in (IV.3), we arrive after integrating over coordinate and momentum variables, and taking the limit $x' \to x$, first at

$$\begin{aligned}\chi_p^{(i)}(x) &= \lim_{x'\to x}\chi_p^{(i)}(x,x') \\ &= i\frac{L_yL_z}{T}\int\frac{\mathcal{D}\bar{p}}{(p_0^2-\omega_p^2)^2}\text{tr}[\gamma^i P_p(x)\,(\gamma\cdot\tilde{p}_p+m)\,P_p(x) \\ &\quad\times\gamma^i P_p(x)\,(\gamma\cdot\tilde{p}_p+m)\,P_p(x)].\end{aligned} \tag{IV.5}$$

Here, L_y and L_z are constant lengths of our probe in second and third spatial directions. They arise from the integration over y and z, respectively. The temperature T in (IV.5) arises from the integration over the compactified imaginary time $\tau \equiv it \in [0,\beta]$, where $\beta = T^{-1}$. Performing then the trace over Dirac matrices, and summing over all Landau levels, we get

$$\chi^{(i)}(x) = 2i\frac{L_yL_z}{T}\sum_{p=0}^{\infty}\int\frac{dp_0dp_2dp_3}{(2\pi)^3}\frac{\mathcal{N}_p^{(i)}}{(p_0^2-\omega_p^2)^2}, \tag{IV.6}$$

where $\omega_p^2 = \tilde{p}_2^2 + p_3 + m^2$ with $\tilde{p}_2^2 = 2eB_0p$ for $eB_0 > 0$ [see (II.17)], and

$$\begin{aligned}\mathcal{N}_p^{(1)} &= 2(p_0^2-\omega_p^2)[f_p^+(x)]^2[f_{p-1}^+(x)]^2, \\ \mathcal{N}_p^{(2)} &= 2(p_0^2-\omega_p^2+\tilde{p}_2^2)[f_p^+(x)]^2[f_{p-1}^+(x)]^2, \\ \mathcal{N}_p^{(3)} &= [p_0^2-\omega_p^2+2(p_3^2-\tilde{p}_2^2)][f_p^+(x)]^4 \\ &\quad+[p_0^2-\omega_p^2+2(p_3^2+\tilde{p}_2^2)][f_{p-1}^+(x)]^4.\end{aligned} \tag{IV.7}$$

Note that in general the contribution in the transverse directions $i = 1,2$ are not equal. However, in the presence of strong magnetic field, where the dynamics of the system is reduced to the lowest Landau level, $p = 0$, and we have therefore

$$\mathcal{N}_0^{(1)} = \mathcal{N}_0^{(2)} = 0, \tag{IV.8}$$

which lead to vanishing electric correlation functions in the transverse directions, i.e. $\chi_0^{\perp} = 0$. As concerns the electric current correlation function in direction parallel to the external magnetic field, $\chi_0^{\|}$, plugging

$$\mathcal{N}_0^{(3)} = (p_0^2-\omega_0^2+2p_3^2)[f_0^+(x)]^4, \tag{IV.9}$$

from (IV.7) in (IV.6), using the definition of $f_0^+(x)$ from (II.16), and integrating over p_2,

$$\int\frac{dp_2}{2\pi}[f_0^+(x)]^4 = \left(\frac{eB_0}{2\pi}\right)^{3/2}, \tag{IV.10}$$

we arrive at

$$\chi_0^{\|} = \frac{2iL_yL_z}{T}\left(\frac{eB_0}{2\pi}\right)^{\frac{3}{2}}\int\frac{dp_0dp_3}{(2\pi)^2}\frac{(p_0^2-\omega_0^2+2p_3^2)}{(p_0^2-\omega_0^2)^2}. \tag{IV.11}$$

Introducing the temperature as in the previous section, and using (III.9) to perform the sum over ℓ, labeling the Matsubara frequencies in

$$\begin{aligned}&\frac{1}{\beta}\sum_{\ell=-\infty}^{\infty}\int\frac{dp_3}{2\pi}\left[\frac{1}{(p_4^2+p_3^2+m^2)} - \frac{2p_3^2}{(p_4^2+p_3^2+m^2)^2}\right] \\ &\quad = \frac{1}{4\pi},\end{aligned} \tag{IV.12}$$

we arrive finally at the components of the electric correlation function in the transverse and longitudinal directions with respect to a constant and strong magnetic field in the LLL approximation

$$\begin{aligned}\chi_0^{\perp} &= 0, \\ \chi_0^{\|} &= \frac{L_yL_z}{2\pi T}\left(\frac{eB_0}{2\pi}\right)^{3/2}.\end{aligned} \tag{IV.13}$$

Note that whereas $\chi_0^{\perp} = 0$, the non-vanishing $\chi_0^{\|}$ does not depend on x, although no integration over x is performed in the definition (IV.3) of $\chi_p^{(i)}(x)$ from (IV.3). To arrive at (IV.13), the result from (IV.12) is used. In the chiral limit $m \to 0$, both integrals appearing on the l.h.s. of (IV.12) are infrared (IR) divergent, and the (bare) fermion mass m, plays the role of an IR regulator. Using the relation (III.9) to expand these integrals in a high-temperature expansion, the IR divergences of the integrals appearing in (IV.12) cancel and we are left with an exact, m independent solution for $\chi_0^{\|}$, which does not also depend on the chemical potential μ. Note that the above result (IV.13) suggests that for $eB_0 \ll T^2$ and $L_yL_z \ll \ell_B^2$ with $\ell_B = (eB_0)^{-1/2}$, apart from $\chi_0^{\perp}$, $\chi_0^{\|}$ also vanishes.

---

[6] The x direction is specified, because of the specific Landau gauge, which fixes A_μ as is described in Sec. II A.

The electric susceptibility of a massless magnetized QED at zero temperature is recently studied in [24]. According to the mechanism of magnetic catalysis [4, 5], in massless QED, the exact chiral symmetry of the original QED Lagrangian is dynamically broken by the external magnetic field. In [24], it is shown that the electric susceptibility in the chirally broken phase at zero temperature is independent of the applied magnetic field. It would be interesting to extend the results presented in [24] to finite temperature and study the temperature dependence of electric susceptibility in chirally broken and symmetric phases of a magnetized QED. This is indeed an open question and we hope to come back to this point in the future.

B. $\chi^{(i)}(u)$ in exponentially decaying magnetic fields

In the case of exponentially decaying magnetic fields, the dimensionless coordinate u plays the same rule as x in the previous section. Thus, defining

$$\chi_\kappa^{(i)}(u,u') = \int \mathcal{D}\hat{x}\mathcal{D}\hat{x}'\mathrm{tr}\big[\gamma^i G_\kappa(\rho,\rho')\gamma^i G_\kappa(\rho',\rho)\big], \tag{IV.14}$$

in analogy to (IV.3), using (II.39) and plugging

$$\begin{aligned} G_\kappa(x,x') &= \xi^2 eB_0 \int \frac{dp_0dp_3}{(2\pi)^2}\, e^{i\bar{p}\cdot(\bar{x}-\bar{x}')} \\ &\quad \times P_n^{2r}(u)\frac{i}{\gamma\cdot\tilde{p}_\kappa - m}P_n^{2r}(u'), \end{aligned} \tag{IV.15}$$

with $P_n^{2r}(x)$ from (II.32) and $\tilde{p}_\kappa$ from (II.37) in (IV.14), we arrive after taking the limit $u' \to u$ at

$$\begin{aligned} \chi_\kappa^{(i)}(u) &= \lim_{u'\to u}\chi_\kappa^{(i)}(u,u') \\ &= \frac{i\alpha^3 L_yL_z}{T}\int\frac{dp_0dp_3}{(2\pi)^2}\frac{1}{(p_0^2-\omega_\kappa^2)^2} \\ &\quad \times \mathrm{tr}[\gamma^i P_n^{2r}(u)\,(\gamma\cdot\tilde{p}_\kappa+m)\,P_n^{2r}(u') \\ &\quad \times \gamma^i P_n^{2r}(u')\,(\gamma\cdot\tilde{p}_\kappa+m)\,P_n^{2r}(u)], \end{aligned} \tag{IV.16}$$

where $\alpha = \xi\sqrt{eB_0}$, $n = s-r$, and, according to (II.37), $\omega_\kappa^2 = \tilde{p}_2^2 + p_3^2 + m^2$ with $\tilde{p}_2^2 = \xi^2 eB_0\kappa$ and $\kappa = s^2 - r^2$. After performing the trace over Dirac matrices, the local electric current correlation function including the contributions of all energy levels reads

$$\chi^{(i)}(u) = \frac{2i\alpha^3 L_yL_z}{T}\sum_{r=1}^{\infty}\sum_{s=r}^{\infty}\int\frac{dp_0dp_3}{(2\pi)^2}\frac{\mathcal{N}_{r,s}^{(i)}}{(p_0^2-\omega_\kappa^2)^2}. \tag{IV.17}$$

For different directions, $i = 1,2,3$, the nominator $\mathcal{N}_{r,s}^{(i)}$ is given by

$$\begin{aligned} \mathcal{N}_{r,s}^{(1)} &= 2(p_0^2-\omega_\kappa^2)[F_n^{2r}(u)]^2[F_{n-1}^{2r}(u)]^2, \\ \mathcal{N}_{r,s}^{(2)} &= 2(p_0^2-\omega_\kappa^2+2\tilde{p}_2^2)[F_n^{2r}(u)]^2[F_{n-1}^{2r}(u)]^2, \\ \mathcal{N}_{r,s}^{(3)} &= [p_0^2-\omega_\kappa^2+2(p_3^2-\tilde{p}_2^2)][F_n^{2r}(u)]^4 \\ &\quad +[p_0^2-\omega_\kappa^2+2(p_3^2+\tilde{p}_2^2)][F_{n-1}^{2r}(u)]^4, \end{aligned} \tag{IV.18}$$

where $F_n^{2r}(u)$ is defined in (II.29). In the LLL, where, according to our explanations in Sec. II B, $s = r$ and therefore $\kappa = 0$, the only contribution to $\chi^{(i)}$ arises from the positive spin particles. We get therefore

$$\mathcal{N}_{r,s=r}^{(1)} = \mathcal{N}_{r,s=r}^{(2)} = 0, \tag{IV.19}$$

leading to vanishing transverse components of the electric current correlation function in the LLL approximation, i.e. $\chi_{\text{LLL}}^{\perp} = 0$. The same effect is also observed in the case of constant magnetic fields in see Sec. IV A. Moreover we get,

$$\mathcal{N}_{r,s=r}^{(3)} = (p_0^2-\omega_0^2+2p_3^2)[F_0^{2r}(u)]^4. \tag{IV.20}$$

Plugging (IV.20) in (IV.17), we arrive first at

$$\begin{aligned} \chi_{\text{LLL}}^{\|}(u) &= \frac{2i\alpha^3 L_yL_z}{T}\sum_{r=1}^{\infty}[F_0^{2r}(u)]^4 \\ &\quad \times \int\frac{dp_0dp_3}{(2\pi)^2}\frac{(p_0^2-\omega_0^2+2p_3^2)}{(p_0^2-\omega_0^2)^2}, \end{aligned} \tag{IV.21}$$

where $\|$ denotes the third (longitudinal) component of $\chi^{(i)}$ in the LLL approximation. In (IV.21), as in Sec. III B, the summation over r can be performed using

$$\begin{aligned} \sum_{r=1}^{\infty}[F_0^{2r}(u)]^4 &= e^{-2u}\sum_{r=1}^{\infty}\left(\frac{u^{2r}}{(2r)!}\right)^2 \\ &= \frac{e^{-2u}}{2}\big[(I_0(2u)+J_0(2u))-2\big], \end{aligned} \tag{IV.22}$$

and $\mathcal{L}_0^{2r} = 1$. Here, $I_0(z)$ and $J_0(z)$ are zeroth order modified Bessel functions I and J. Plugging (IV.22) in (IV.21), we arrive at

$$\begin{aligned} \chi_{\text{LLL}}^{\|}(u) &= \frac{i\alpha^3 L_yL_z}{T}e^{-2u}\big[(I_0(2u)+J_0(2u))-2\big] \\ &\quad \times \int\frac{dp_0dp_3}{(2\pi)^2}\frac{(p_0^2-\omega_0^2+2p_3^2)}{(p_0^2-\omega_0^2)^2}. \end{aligned} \tag{IV.23}$$

Introducing the temperature and finite density, using the method introduced in the previous section, and using (IV.12) to perform the integration over p_3 and the sum over the Matsubara frequencies, the transverse and longitudinal components of the local electric current correlation function in the LLL approximation read

$$\begin{aligned}\chi^{\perp}_{\text{LLL}} &= 0,\\ \chi^{\parallel}_{\text{LLL}}(u) &= \frac{\xi^3(eB_0)^{3/2}\ L_yL_z}{4\pi T}\\ &\quad\times e^{-2u}\big[I_0(2u)+J_0(2u)-2\big].\quad \text{(IV.24)}\end{aligned}$$

In the next section, we will compare local electric current correlation functions (IV.13) and (IV.24) arising from constant and exponentially decaying magnetic fields, and discuss the remarkable property of (IV.24) in the limit $\xi \to 0$.

V. DISCUSSIONS

In the previous sections, the chiral condensate $\langle\bar{\psi}\psi\rangle$ and local electric current correlation function $\chi^{(i)}$ are computed in the presence of constant and exponentially decaying magnetic fields in the LLL approximation. As it turns out the transverse ($i = 1, 2$) components of $\chi^{(i)}$ vanish in this approximation. Moreover, whereas in the presence of constant and strong magnetic fields $\langle\bar{\psi}\psi\rangle^c_{\text{LLL}}$ from (III.6) and $\chi^{\parallel}_0$ from (IV.13) are constant (as a function of coordinates), they depend, in the presence of exponentially decaying magnetic fields, on a variable u defined by $u = \frac{2}{\xi^2}e^{-\xi\eta}$. Here, η is proportional to the coordinate x, and is given explicitly by $\eta = x/\ell_B$, where the magnetic length $\ell_B = (eB_0)^{-1/2}$. To give an explicit example on η, let us take $eB_0 = 15m_\pi^2 \sim 0.3$ GeV^2, with the pion mass $m_\pi \sim 140$ MeV. This corresponds to a magnetic field $B_0 \sim 5\times 10^{19}$ Gauß,[7] which is the typical magnetic field produced in the early stages of heavy ion collisions at LHC [26] or exists in the interior of compact stars [27]. In this case, the corresponding magnetic length is given by $\ell_B \sim 0.4$ fm.[8] Taking $\eta = 4$, for instance, would mean a distance $x = 4\ell_B \sim 1.6$ fm from the origin at $x = 0$, etc. Note that for the above mentioned LLL approximation to be reliable, we have to consider only small damping parameter ξ and consider the probe in small η from the origin $x = 0$ with $B(x = 0) = B_0$.

In this section, we will compare the values of $\langle\bar{\psi}\psi\rangle^c_{\text{LLL}}$ from (III.6) with $\langle\bar{\psi}\psi\rangle_{\text{LLL}}$ from (III.14), as well as $\chi^{(i)}_0$ from (IV.13) with $\chi^{(i)}_{\text{LLL}}$ from (IV.24), in order to explore the effect of inhomogeneity of the external magnetic field, especially once quantum corrections are taken into account. To do this, let us first define the ratio

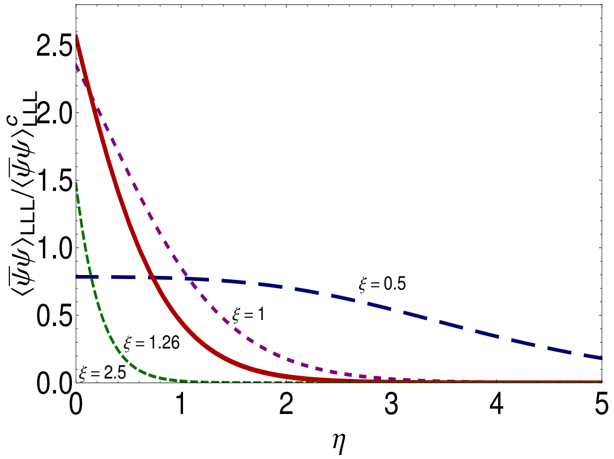

FIG. 1: The ratio $\mathcal{C}_\xi(\eta) = \langle\bar{\psi}\psi\rangle_{\text{LLL}}/\langle\bar{\psi}\psi\rangle^c_{\text{LLL}}$ is plotted as a function of $\eta = x/\ell_B$ with $\ell_B = (eB_0)^{-1/2}$ for different damping parameters $\xi = 0.5, 1, 1.26, 2.5$. The condensates $\langle\bar{\psi}\psi\rangle_{\text{LLL}}$ and $\langle\bar{\psi}\psi\rangle^c_{\text{LLL}}$ are defined in (III.14) and (III.6), respectively. For the damping factor $\xi \sim 1.26$, the ratio $\mathcal{C}_\xi(\eta)$ is maximized at $\eta = 0$ (or equivalently $x = 0$).

$$\mathcal{C}_\xi(\eta) \equiv \frac{\langle\bar{\psi}\psi\rangle_{\text{LLL}}}{\langle\bar{\psi}\psi\rangle^c_{\text{LLL}}} = 2\pi\xi^2 e^{-u}\left(\cosh(u) - 1\right), \quad \text{(V.1)}$$

with $u = \frac{2}{\xi^2}e^{-\xi\eta}$ and $\eta = x/\ell_B$.

In Fig. 1, $\mathcal{C}_\xi(\eta)$ is plotted for different damping parameters $\xi = 0.5, 1, 1.26, 2.5$ as a function of $\eta = x/\ell_B$. Depending on the damping parameter ξ, the condensate $\langle\bar{\psi}\psi\rangle_{\text{LLL}}$ arising from an exponentially decaying magnetic field is up to a factor 2.5 greater than the condensate $\langle\bar{\psi}\psi\rangle^c_{\text{LLL}}$ in the presence of a uniform magnetic field. For $\xi \sim 1.26$ the maximum value of the condensate $\langle\bar{\psi}\psi\rangle_{\text{LLL}}$ arises at $\eta = 0$ or equivalently at $x = 0$. Let us notice that this interesting observation is indeed in contradiction to our prior expectation, according to which we expect $\mathcal{C}_\xi(\eta) = 1$ at $\eta = 0$ (or equivalently at $x = 0$), because $B(x = 0) = B_0$ is constant. This indicates the singular nature of $\eta = 0$ (or equivalently $x = 0$), once quantum fluctuations produce a nonvanishing chiral condensate $\langle\bar{\psi}\psi\rangle$.

The singular nature of $\mathcal{C}_\xi(\eta)$ for $\xi = 0$ is explored in Fig. 2, where the same ratio $\mathcal{C}_\xi(\eta)$ is plotted as a function of the damping factor ξ for $\eta = 0, 0.5, 1, 2$ (or equivalently for $x = 0, \ell_B/2, \ell_B, 2\ell_B$). For $\eta = 0$, $\mathcal{C}_\xi(0)$ is maximized at $\xi \sim 1.26$. For $\eta \neq 0$, however, the maxima of $\mathcal{C}_\xi(\eta)$ are shifted to smaller values of ξ. At $\xi = 0$, the condensate $\langle\bar{\psi}\psi\rangle_{\text{LLL}}$, arising from an exponentially decaying magnetic field, vanishes for all demonstrated values of η. This is again in contradiction to our prior expectation, according to which we expect $\mathcal{C}_\xi(\eta) = 1$ for $\xi = 0$. This is because for $\xi = 0$ the exponentially decaying magnetic field

---

[7] We are working in the units where $eB = 1$ GeV^2 corresponds to $B_0 \sim 1.7\times 10^{20}$ Gauß [25].

[8] As it turns out, the magnetic length ℓ_B for $eB_0 = 1$ GeV^2 is given by $\ell_B \sim 0.63$ fm.

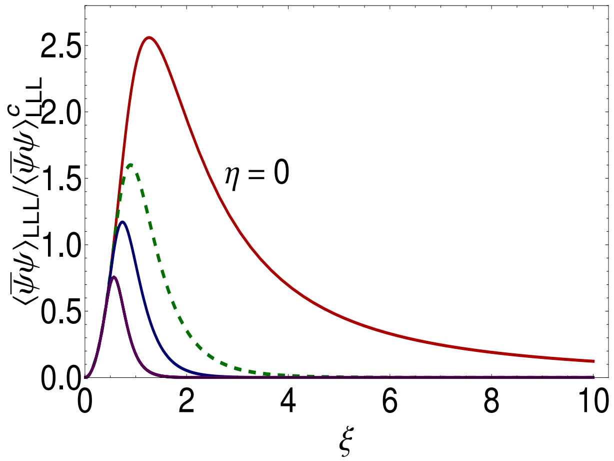

FIG. 2: The ratio $\mathcal{C}_\xi(\eta) = \langle\bar{\psi}\psi\rangle_{\rm LLL}/\langle\bar{\psi}\psi\rangle^{c}_{\rm LLL}$ from (V.1) is plotted as a function of the damping factor ξ for $\eta = 0, 0.5, 1, 2$ (or equivalently for $x = 0, \ell_B/2, \ell_B, 2\ell_B$ with $\ell_B = (eB_0)^{-1/2}$) from above to below. For $\eta = 0$, the $\mathcal{C}_\xi(\eta)$ is maximized at $\xi \sim 1.26$. For $\eta \neq 0$ (or equivalently $x \neq 0$), the maxima are shifted to smaller values of ξ. For all values of η, the condensate $\langle\bar{\psi}\psi\rangle_{\rm LLL}$, arising from an exponentially decaying magnetic field, vanishes at $\xi = 0$.

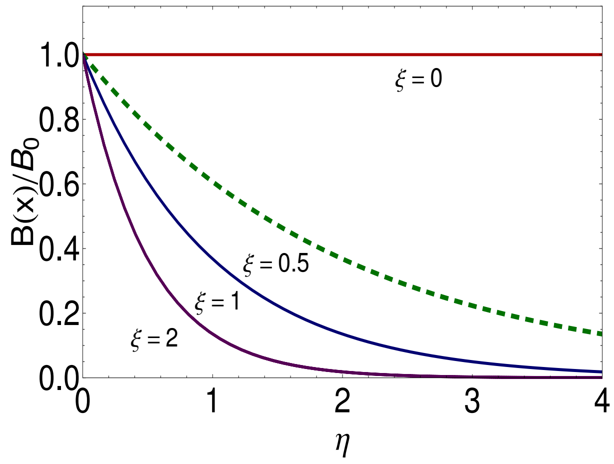

FIG. 3: The ratio $B(x)/B_0 = e^{-\eta\xi}$ with $\eta = x/\ell_B$ and $\ell_B = (eB_0)^{-1/2}$, is plotted as a function of the damping factor η for $\xi = 0, 0.5, 1, 2$ from above to below.

$B(x) = B_0 e^{-\xi\eta}$ becomes constant (see Fig. 3).

The same singular behavior at $\eta = 0$ and $\xi = 0$ is also observed when we repeat the above analysis for the ratio

$$\chi_\xi(\eta) \equiv \frac{\chi^{\|}_{\rm LLL}(u)}{\chi^{\|}_{0}} = \sqrt{2\pi^3}\xi^3 e^{-2u}[I_0(2u) + J_0(2u) - 2], \quad \text{(V.2)}$$

where $\chi^{\|}_0$ from (IV.13) and $\chi^{\|}_{\rm LLL}(u)$ from (IV.24) are local electric current correlation functions in the presence of a uniform and an exponentially decaying magnetic fields, respectively. Here, as before, $u = \frac{2}{\xi^2}e^{-\xi\eta}$ and $\eta = x/\ell_B$, with $\ell_B = (eB_0)^{-1/2}$.

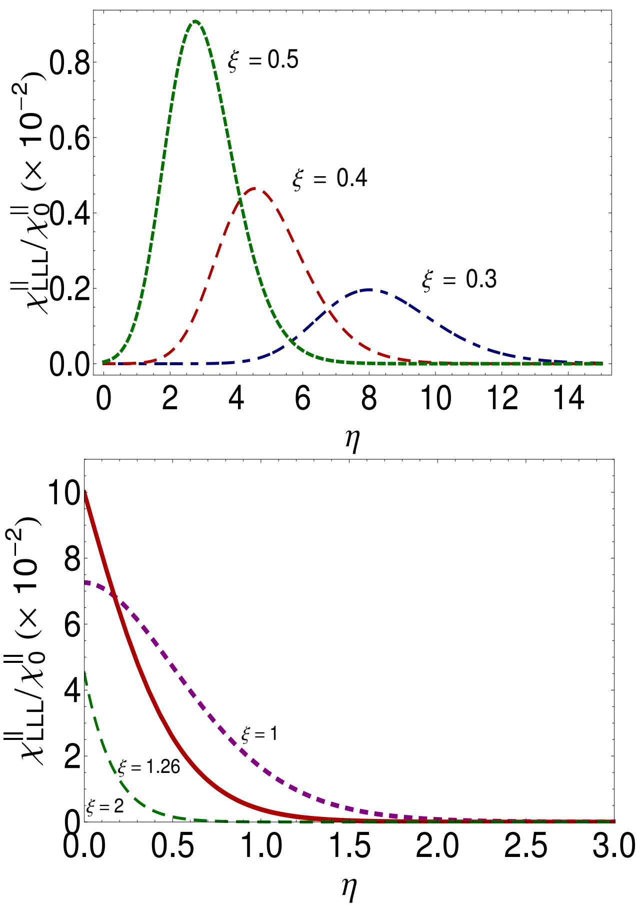

FIG. 4: The ratio $\chi_\xi(\eta) = \chi^{\|}_{\rm LLL}(u)/\chi^{\|}_0$ from (V.2) is plotted as a function of $\eta = x/\ell_B$ with $\ell_B = (eB_0)^{-1/2}$ for different damping parameters $\xi = 0.1, 0.2, \cdots, 1, 1.26, 2$. For $\xi \sim 1.26$, the ratio $\chi_\xi(\eta)$ is maximized at $\eta = 0$.

In Fig. 4, the ratio $\chi_\xi(\eta)$ is plotted for $\xi = 0.3, 0.4, \cdots, 2$ as a function of η. The fact that $\chi_\xi(\eta) \neq 1$ for $\eta = 0$ is again in contradiction to our prior expectation: We know that the x-dependent magnetic field $B(x) = B_0 e^{-\eta\xi}$ becomes constant for $\eta = 0$ (or equivalently $x = 0$), and therefore the prior expectation is that $\chi_\xi(\eta) = 1$ as well as $\mathcal{C}_\xi(\eta) = 1$ for $\eta = 0$. The above observation demonstrates again the singular nature of the limit $x \to 0$, once the quantum effects are to be considered. Another remarkable point here is that, according to Fig. 2, for $\eta = 0$ (or equivalently $x = 0$) and in the interval $0.5 \lesssim \xi \lesssim 4$, the ratio $\mathcal{C}_\xi(\eta) \geq 1$, whereas according to Fig. 4 (see also Fig. 5), $\chi_\xi(\eta) \leq 1$ for $\eta = 0$ and in the same interval $0.5 \lesssim \xi \lesssim 4$. In other words, for $\eta = 0$ and in the interval $0.5 \lesssim \xi \lesssim 4$,[9] the value of the electric current correlation function $\chi_0^{\parallel}$ arising from a constant magnetic field is always larger than $\chi_{\text{LLL}}^{\parallel}(u)$ arising from an exponentially decaying magnetic field, whereas in the same interval of ξ, $\langle\bar{\psi}\psi\rangle_{\text{LLL}}^{c}$ arising from a constant magnetic field is always smaller than $\langle\bar{\psi}\psi\rangle_{\text{LLL}}$ arising from an exponentially decaying magnetic field.

In Fig. 5, the same ratio $\chi_{\xi}(\eta)$ from (V.2) is plotted as a function of the damping factor ξ for fixed $\eta = 0, 0.5, 1, 2$ (or equivalently for $x = 0, \ell_B/2, \ell_B, 2\ell_B$ with $\ell_B = (eB_0)^{-1/2}$) from above to below. As it turns out the value of $\chi_{\text{LLL}}^{\parallel}(u)$ for $\xi \to 0$ vanishes, in contrast to our expectation.

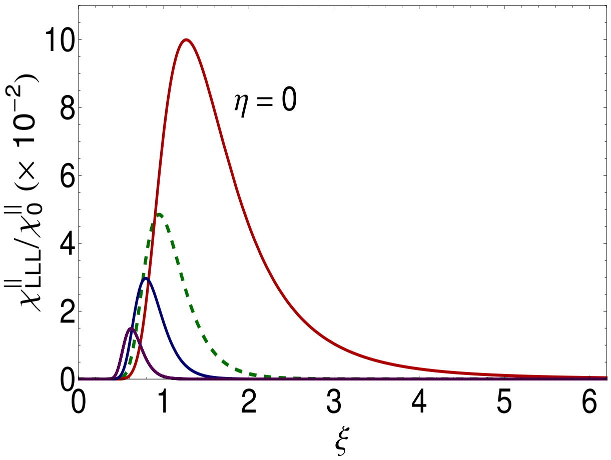

FIG. 5: The ratio $\chi_{\xi}(\eta)$ from (V.2), is plotted as a function of the damping factor ξ for $\eta = 0, 0.5, 1, 2$ (or equivalently for $x = 0, \ell_B/2, \ell_B, 2\ell_B$ with $\ell_B = (eB_0)^{-1/2}$) from above to below. For $\eta = 0$, $\chi_{\xi}(\eta)$ is maximized at $\xi \sim 1.26$. For $\eta \neq 0$ (or equivalently $x \neq 0$), the maxima are shifted to smaller values of ξ. For all values of η, $\chi_{\text{LLL}}^{\parallel}(u)$ vanishes at $\xi = 0$.

The second observation from Fig. 5 is that the maxima of $\chi_{\xi}(\eta)$ are shifted to smaller values of ξ for increasing η. In Fig. 6, the values of ξ that maximize the ratios defined in (V.1) [blue circles] and (V.2) [green rectangles] are plotted as a function of η. They are almost the same. This indicates a certain relation between the formation of chiral condensates and the value of electric current correlation function in a system including relativistic fermions.

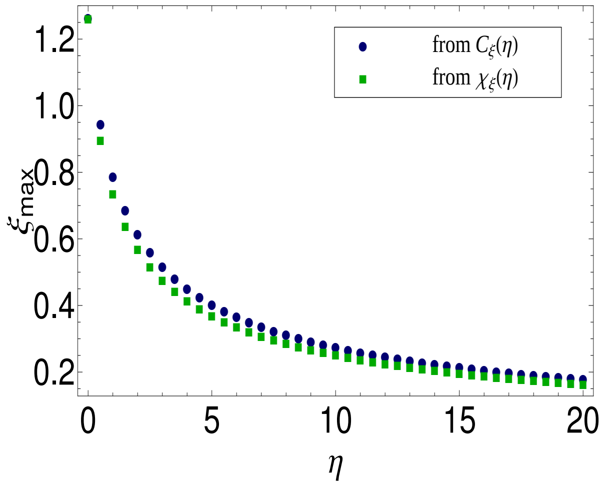

FIG. 6: The values of ξ that maximize the ratios $\mathcal{C}_{\xi}(\eta)$ from (V.1) [blue circles] and $\chi_{\xi}(\eta)$ from (V.2) [green rectangles] are plotted as a function of η. They almost overlap.

This relation is demonstrated in Figs. 7a-7c, where $\chi_{\xi}(\eta)$ from (V.2) is plotted as a function of $\mathcal{C}_{\xi}(\eta)$ from (V.1) for fixed $\eta = 0, 0.2, 0.5, 1$ (or equivalently, $x = 0, \ell_B/5, \ell_B/2, \ell_B$) and various damping parameters $\xi = 0.1, \cdots, 10$. Each dot in Figs. 7a-7c indicates a value of $\xi = 0.1, \cdots, 10$ with $\Delta\xi = 0.05$. As it turns out, $\chi_{\xi}(\eta)$ increases with increasing $\mathcal{C}_{\xi}(\eta)$ for a certain numbers of ξ (see Fig. 7a). The maximum value of ξ for which this is true, is different for different η. Let us denote this specific ξ with $\xi_{\star}$. For $\eta = 0, 0.2, 0.5, 1$, $\xi_{\star}$'s are $\xi_{\star} \sim 1.3, 1.1, 0.95, 0.3$, respectively. For $\xi > \xi_{\star}$, however, $\chi_{\xi}(\eta)$ decreases with decreasing $\mathcal{C}_{\xi}(\eta)$ (see Fig. 7b). In Fig. 7c, the two curves in Fig. 7a and 7b are reassembled and demonstrate a hysteresis-like curve with increasing ξ. However, since the LLL approximation is only valid for small ξ and η, we shall limit us to the values of $\xi \leq \xi_{\star}$ for which $\chi_{\xi}(\eta)$ increases with increasing $\mathcal{C}_{\xi}(\eta)$ (Fig. 7a).

VI. CONCLUDING REMARKS

In the present paper, the effect of exponentially decaying magnetic fields on the dynamics of Dirac fermions is explored in detail. Using the Ritus eigenfunction method, we have first determined the energy spectrum of fermions in this non-uniform magnetic field and compared it with the energy spectrum of relativistic fermions in a constant magnetic field. We have then computed the chiral condensate $\langle\bar{\psi}\psi\rangle$ and local electric current correlation function $\chi^{(i)}$ in the presence of strong uniform and non-uniform magnetic fields in the LLL approximation. In non-uniform magnetic fields, $\langle\bar{\psi}\psi\rangle$ and $\chi^{(i)}$ depend on a dimensionless variable $u = \frac{2}{\xi^2}e^{-\xi x/\ell_B}$, which is a nontrivial function of the magnetic field's damping parameter ξ, the coordinate x and the magnetic length $\ell_B = (eB_0)^{-1/2}$.

---

[9] As before mentioned, the LLL approximation is only reliable for small values of ξ and η.

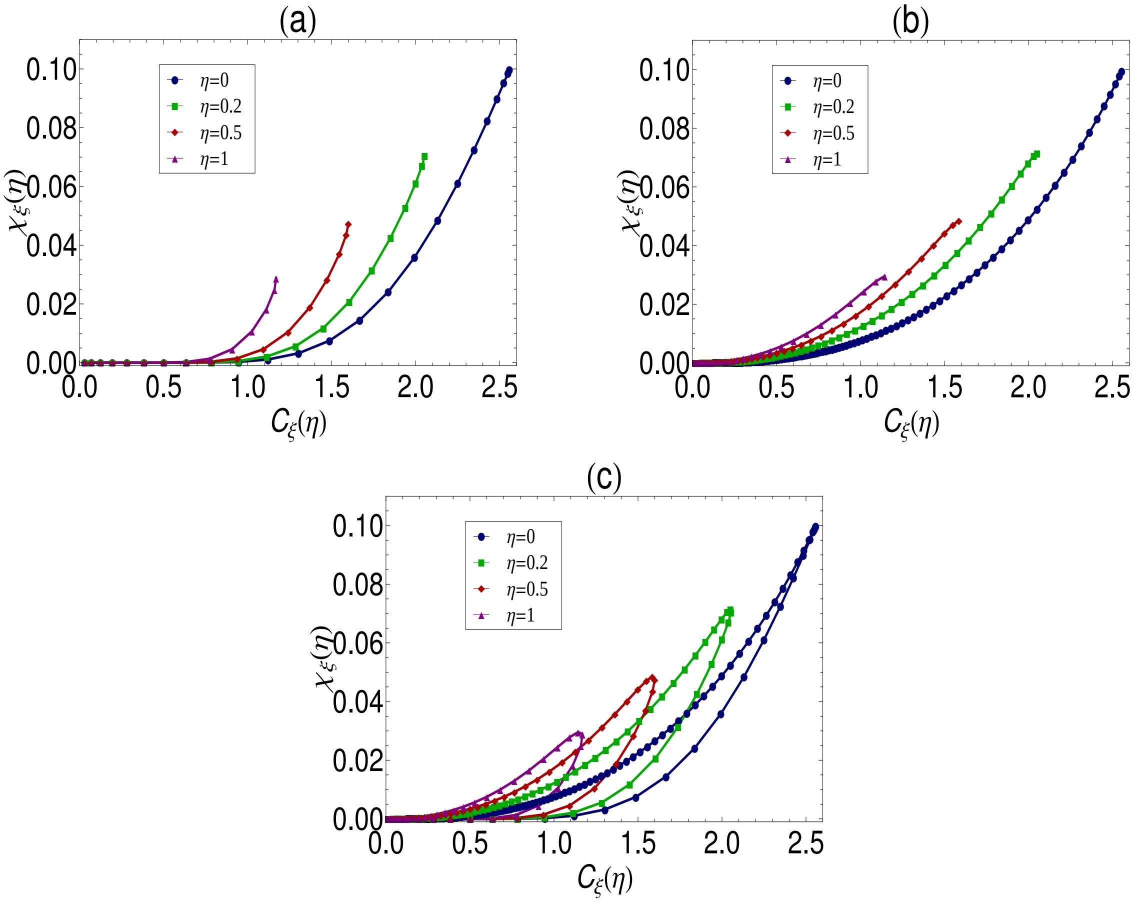

FIG. 7: The ratio $\chi_\xi(\eta)$ from (V.2) is plotted as a function of the ratio $\mathcal{C}_\xi(\eta)$ from (V.1) for fixed $\eta = 0, 0.2, 0.5, 1$ (or equivalently, $x = 0, \ell_B/5, \ell_B/2, \ell_B$) and various damping parameters $\xi = 0.1, \cdots, 10$. Each dot in the above curves indicates a value of $\xi = 0.1, \cdots, 10$ with $\Delta\xi = 0.05$. For ξ smaller than a certain $\xi_\star$, $\chi_\xi(\eta)$ increases with increasing $\mathcal{C}_\xi(\eta)$ (panel a). The value of $\xi_\star$ is different for different η (see the main text). For $\xi > \xi_\star$, however, $\chi_\xi(\eta)$ decreases with decreasing $\mathcal{C}_\xi(\eta)$ (panel b). The two curves in panels a and b are reassembled in panel c. In the LLL approximation, for small values of ξ and η, only the behavior demonstrated in panel a is relevant.

In the LLL approximation, the transverse components of the electric susceptibility, $\chi^{(i)}_{\text{LLL}}, i = 1, 2$, vanish and its longitudinal component $\chi^{\parallel}_{\text{LLL}}$ depends also on the variable u, only in the presence of exponentially decaying magnetic fields. We have shown that the limits $\xi \to 0$ as well as $x \to 0$ are singular. In these limits, the x-dependent magnetic field becomes constant, and therefore $\langle\bar{\psi}\psi\rangle_{\text{LLL}}$ as well as $\chi^{\parallel}_{\text{LLL}}$ arising from the x-dependent magnetic field are expected to have the same value as in a constant magnetic field. But, as it turns out this is not the case. This remarkable behavior of $\langle\bar{\psi}\psi\rangle_{\text{LLL}}$ as well as $\chi^{\parallel}_{\text{LLL}}$ at $\xi \to 0$ and/or $x \to 0$ is discussed in detail in Sec. V. Let us notice that, mathematically, there is a difference between taking the limit of a quantity to zero and setting it exactly equal to zero. This difference is indeed responsible for the singular behavior of the limits $\xi \to 0$ and/or $x \to 0$. When we are looking for the solution of the differential equation (II.22) for non-uniform magnetic fields, for instance, the parameter ξ appearing in $u = \frac{2}{\xi^2} e^{-\xi\sqrt{eB_0}x}$ can be very small ($\xi \to 0$), but it cannot be set exactly equal to zero. When $\xi = 0$, the magnetic field becomes constant, and the differential equation (II.22), leading to the solution (II.31), including associated Laguerre polynomials, has to be replaced by the differential equation (II.13) for constant magnetic fields, leading to Hermite polynomials. There is no way to reproduce the Hermite solution of the latter case from the associated Laguerre solution of the former case, by taking $\xi \to 0$. This is why that although at the classical level the uniform magnetic field is reproduced in these limits from the non-uniform magnetic field, neither the energy spectrum nor the quantum corrections to $\langle\bar{\psi}\psi\rangle_{\text{LLL}}$ as well as $\chi^{\parallel}_{\text{LLL}}$ of the constant magnetic fields can be reproduced from their values in the non-uniform magnetic

$n > n'$ and $r' > r$				$n > n'$ and $r' < r$	
$n - n' > r' - r$	$n - n' = r' - r$	$n - n' < r' - r \leq n$	$n < r' - r$	$r - r' \leq n'$	$r - r' > n'$
I_1	I_2	I_3	I_4	I_5	I_6

TABLE I: The integrals $I_i, i = 1, \cdots, 6$ are presented in (A.3) and (A.4).

field by taking the limit $\xi \to 0$.

We have also shown that for small values of x/ℓ_B and ξ, where we believe that the LLL approximation is reliable, the ratio $\chi_\xi(\eta)$ from (V.2) increases with increasing ratio $\mathcal{C}_\xi(\eta)$ from (V.1) up to a maximum value of ξ, denoted by $\xi_\star$. As it turns out, the value of $\xi_\star$ depends on η (see Sec. V).

Let us notice that electric susceptibility (electric current correlation function) of a three-flavor color superconductor is recently computed in a strong homogeneous magnetic field in [28], and the magnetoelectric effect in a strongly magnetized quark matter is studied in detail. The present work is a second nontrivial example on the effect of external magnetic fields, in general, and spatially decaying magnetic fields, in particular, on electric current correlation function of a system containing relativistic Dirac fermions. Apart from applications in condensed matter physics, the results of this paper may also be relevant in the context of heavy ion collisions. Here, recent experimental activities at RHIC indicate the production of intense magnetic fields in the early stage of non-central heavy ion collisions [26]. Depending on the initial conditions, e.g. the energy of colliding nucleons and the corresponding impact parameters, the spatially varying magnetic fields are estimated to be in the order of $B \sim 10^{18} - 10^{19}$ Gauß, decaying very fast, within few femtometers to $B \sim 10^{13} - 10^{14}$ Gauß, and vanishing during the hadronization process [26].

VII. ACKNOWLEDGMENTS

The authors acknowledge valuable discussions with Sh. Fayazbakhsh, S. A. Jafari and A. Vaezi.

Appendix A: Orthonormality relations of associated Laguerre polynomials

In this appendix, we present a number of useful orthonormality relations of associated Laguerre polynomials. To do this, let us define the integral

$$I_{n,n'}^{r,r'} = \int_0^\infty du\ e^{-u} u^{r+r'} \mathcal{L}_n^{2r}(u) \mathcal{L}_{n'}^{2r'}(u). \qquad (A.1)$$

For $r = r'$, the standard orthonormality relation of associated Laguerre polynomials is given by

$$I_{n,n'}^{r,r} = \frac{(n+2r)!}{n!} \delta_{n,n'}. \qquad (A.2)$$

But, in the present paper, we have to consider the cases, where in general $r \neq r'$. To determine $I_{n,n'}^{r,r'}$, we have to distinguish several cases, which are summarized in Tables I and II.

$n < n'$ and $r' < r$				$n < n'$ and $r' > r$	
$n' - n > r - r'$	$n' - n = r - r'$	$n' - n < r - r' \leq n'$	$n' < r - r'$	$r' - r < n$	$r' - r \geq n$
I_7	I_8	I_9	I_{10}	I_{11}	I_{12}

TABLE II: The integrals $I_i, i = 7, \cdots, 12$ are presented in (A.5) and (A.6).

The integrals $I_i, i = 1, \cdots, 4$ for $n > n'$ and $r' > r$ are given by

$$\begin{aligned}
I_1 &= 0, \\
I_2 &= \frac{(-1)^{r'-r}\ (r'+r+n')!}{n'!}, \\
I_3 &= \sum_{\ell=0}^{(r'-r)-(n-n')} \frac{(-1)^{n-n'+\ell}\ (r'-r)(r'+r+\ell-n')!\ (r'-r+\ell-1)!}{\ell!\ (n'-\ell)!\ (n-n'+\ell)!\ (r'-r-n+n'-\ell)!}, \\
I_4 &= \sum_{\ell=0}^{n'} \frac{(-1)^{n-n'+\ell}(r'-r)(r'+r+\ell-n')!(r'-r+\ell-1)!}{\ell!\ (n'-\ell)!\ (n-n'+\ell)!\ (r'-r-n+n'-\ell)!}.
\end{aligned} \qquad (A.3)$$

For $n > n'$ and $r' < r$, we have

$$\begin{aligned} I_5 &= \sum_{\ell=0}^{r-r'} \frac{(-1)^\ell (r-r')(r'+r+n'-\ell)!(r-r'+n-n'+\ell-1)!}{\ell!\,(n'-\ell)!(n-n'+\ell)!(r-r'-\ell)!}, \\ I_6 &= \sum_{\ell=0}^{n'} \frac{(-1)^\ell (r-r')(r'+r+n'-\ell)!(r-r'+n-n'+\ell-1)!}{\ell!\,(n'-\ell)!(n-n'+\ell)!(r-r'-\ell)!}. \end{aligned} \tag{A.4}$$

The integrals $I_i, i = 7, \cdots, 10$ for $n < n'$ and $r' < r$ are given by

$$\begin{aligned} I_7 &= 0, \\ I_8 &= \frac{(-1)^{r-r'}\,(r'+r+n)!}{n!}, \\ I_9 &= \sum_{\ell=0}^{(r-r')-(n'-n)} \frac{(-1)^{n'+\ell-n}\,(r-r')(r+r'-n+\ell)!\,(r-r'+\ell-1)!}{\ell!\,(n-\ell)!\,(n'-n+\ell)!\,(r-r'-n'+n-\ell)!}, \\ I_{10} &= \sum_{\ell=0}^{n} \frac{(-1)^{n'-n+\ell}(r-r')(r+r'+\ell-n)!(r-r'+\ell-1)!}{\ell!\,(n-\ell)!\,(n'-n+\ell)!\,(r-r'-n'+n-\ell)!}. \end{aligned} \tag{A.5}$$

For $n < n'$ and $r' > r$, we get

$$\begin{aligned} I_{11} &= \sum_{\ell=0}^{r'-r} \frac{(-1)^\ell (r'-r)(r'+r+n-\ell)!(r'-r+n'-n+\ell-1)!}{\ell!\,(n-\ell)!(n'-n+\ell)!(r'-r-\ell)!}, \\ I_{12} &= \sum_{\ell=0}^{n} \frac{(-1)^\ell (r'-r)(r'+r+n-\ell)!(r'-r+n'-n+\ell-1)!}{\ell!\,(n-\ell)!(n'-n+\ell)!(r'-r-\ell)!}. \end{aligned} \tag{A.6}$$

[1] V. C. Zhukovsky, K. G. Klimenko, V. V. Khudyakov and D. Ebert, *Magnetic catalysis of parity breaking in a massive Gross-Neveu model and high-temperature superconductivity*, JETP Lett. **73**, 121 (2001) [Pisma Zh. Eksp. Teor. Fiz. **73**, 137 (2001)], arXiv: hep-th/0012256.
E. J. Ferrer, V. P. Gusynin and V. de la Incera, *Magnetic field induced gap and kink behavior of thermal conductivity in cuprates*, Mod. Phys. Lett. B **16**, 107 (2002), arXiv: hep-ph/0101308.
E. V. Gorbar, V. P. Gusynin, V. A. Miransky and I. A. Shovkovy, *Dynamics in the quantum Hall effect and the phase diagram of graphene*, Phys. Rev. B **78**, 085437 (2008), arXiv:0806.0846 [cond-mat.mes-hall].

[2] K. G. Klimenko and V. C. Zhukovsky, *Does there arise a significant enhancement of the dynamical quark mass in a strong magnetic field?*, Phys. Lett. B **665**, 352 (2008), arXiv:0803.2191 [hep-ph].
A. Ayala, A. Bashir, E. Gutierrez, A. Raya and A. Sanchez, *Chiral and parity symmetry breaking for planar fermions: Effects of a heat bath and uniform external magnetic field*, Phys. Rev. D **82**, 056011 (2010), arXiv:1007.4249 [hep-ph].
I. E. Frolov, V. C. Zhukovsky and K. G. Klimenko, *Chiral density waves in quark matter within the Nambu–Jona-Lasinio model in an external magnetic field*, arXiv:1007.2984 [hep-ph].
E. V. Gorbar, V. A. Miransky and I. A. Shovkovy, *Chiral asymmetry and axial anomaly in magnetized relativistic matter*, Phys. Lett. B **695**, 354 (2011), arXiv:1009.1656 [hep-ph].
S. Fayazbakhsh and N. Sadooghi, *Phase diagram of hot magnetized two-flavor color superconducting quark matter*, Phys. Rev. D **83**, 025026 (2011), arXiv:1009.6125 [hep-ph]; *ibid.*, *Color neutral 2SC phase of cold and dense quark matter in the presence of constant magnetic fields*, *ibid.* **82**, 045010 (2010), arXiv:1005.5022 [hep-ph].
R. Gatto and M. Ruggieri, *Deconfinement and chiral symmetry restoration in a strong magnetic background*, Phys. Rev. D **83**, 034016 (2011), arXiv:1012.1291 [hep-ph].
V. V. Braguta, P. V. Buividovich, M. N. Chernodub and M. I. Polikarpov, *Electromagnetic superconductivity of vacuum induced by strong magnetic field: numerical evidence in lattice gauge theory*, arXiv:1104.3767 [hep-lat].
F. Preis, A. Rebhan and A. Schmitt, *Holographic baryonic matter in a background magnetic field*, arXiv:1109.6904 [hep-th].

M. N. Chernodub, J. Van Doorsselaere and H. Verschelde, *Electromagnetically superconducting phase of vacuum in strong magnetic field: structure of superconductor and superfluid vortex lattices in the ground state*, Phys. Rev. D **85**, 045002 (2012), arXiv:1111.4401 [hep-ph].

E. S. Fraga and L. F. Palhares, *Deconfinement in the presence of a strong magnetic background: an exercise within the MIT bag model*, arXiv:1201.5881 [hep-ph].

S. S. Avancini, D. P. Menezes, M. B. Pinto and C. Providencia, *The QCD critical end point under strong magnetic fields*, arXiv:1202.5641 [hep-ph].

M. G. de Paoli and D. P. Menezes, *Particle yields in heavy ion collisions and the influence of strong magnetic fields*, arXiv:1203.3175 [nucl-th].

E. -M. Ilgenfritz, M. Kalinowski, M. Muller-Preussker, B. Petersson and A. Schreiber, *Two-color QCD with staggered fermions at finite temperature under the influence of a magnetic field*, arXiv:1203.3360 [hep-lat].

[3] E. Elizalde, E. J. Ferrer and V. de la Incera, *Neutrino propagation in a strongly magnetized medium*, Phys. Rev. D **70**, 043012 (2004), arXiv: hep-ph/0404234.

E. J. Ferrer and V. de la Incera, *Neutrino propagation and oscillations in a strong magnetic field*, Int. J. Mod. Phys. A **19**, 5385 (2004), arXiv: hep-ph/0408108.

E. Bavarsad, M. Haghighat and R. Mohammadi, *Nucleon-nucleon scattering in a strong external magnetic field and the meutrino emissivity*, Phys. Rev. D **82**, 105015 (2010), arXiv:1010.3906 [hep-ph].

J. Alexandre, J. Ellis and N. E. Mavromatos, *On the possibility of superluminal neutrino propagation*, Phys. Lett. B **706**, 456 (2012), arXiv:1109.6296 [hep-ph].

[4] K. G. Klimenko, *Three-dimensional Gross-Neveu model at nonzero temperature and in an external magnetic field*, Z. Phys. C **54**, 323 (1992).

[5] V. P. Gusynin, V. A. Miransky and I. A. Shovkovy, *Dimensional reduction and catalysis of dynamical symmetry breaking by a magnetic field*, Nucl. Phys. **B462**, 249 (1996), arXiv: hep-ph/9509320.

[6] A. De Martino, L. Dell'Anna and R. Egger, *Magnetic confinement of massless Dirac fermions in graphene* Phys. Rev. Lett. **98**, 066802 (2007), arXiv:cond-mat/0610290 [cond-mat.mes-hall].

[7] A. Kormanyos, P. Rakyta, L. Oroszlany and J. Cserti, *Bound states in inhomogeneous magnetic field in graphene: a semiclassical approach*, Phys. Rev. B **78**, 045430 (2008), arXiv:0805.2527 [cond-mat.mes-hall].

[8] P. Roy, T. Kanti Ghosh, K. Bhattacharya, *Localization of Dirac-like excitations in graphene in the presence of smooth inhomogeneous magnetic fields*, J. Phys.: Cond. Mat. **24**, 055301 (2012), arXiv:1108.1907 [cond-mat.mes-hall].

[9] M. Ramezani Masir, P. Vasilopoulos, A. Matulis and F. M. Peeters, *Direction-dependent tunneling through nanostructured magnetic barriers in graphene*, Phys. Rev. B **77**, 235443 (2008).

P. Rakyta, L. Oroszlany, A. Kormanyos, C. J. Lambert and J. Cserti, *Peculiar nature of snake states in graphene*, Phys. Rev. B **77**, 081403 (R) (2008), arXiv:0707.3974 [cond-mat.mes-hall].

L. Dell Anna and A. De Martino, *Magnetic superlattice and finite-energy Dirac points in graphene*, Phys. Rev. B **83**, 155449 (2011), arXiv:1101.1918 [cond-mat.mes-hall].

[10] E. Milpas, M. Torres and G. Murguia, *Magnetic field barriers in graphene: an analytically solvable model*, arXiv:1102.5298 [cond-mat.mes-hall].

[11] K. Handrich, *Quantum mechanical magnetic-field-gradient drift velocity: An analytically solvable model*, Phys. Rev. B **72**, 161308 (2005).

[12] T. K. Ghosh, *Exact solutions for a Dirac electron in an exponentially decaying magnetic field*, J. Phys.: Cond. Mat. **21**, 045505 (2009), arXiv:0911.5622 [cond-mat.mes-hall].

[13] A. Raya, E. Reyes, *Fermion condensate and vacuum current density induced by homogeneous and inhomogeneous magnetic fields in (2+1)-dimensions*, Phys. Rev. D **82**, 016004 (2010), arXiv:1006.2548 [hep-ph].

[14] H. Gies and L. Roessler, *Vacuum polarization tensor in inhomogeneous magnetic fields*, Phys. Rev. D **84**, 065035 (2011), arXiv:1107.0286 [hep-ph].

[15] V. I. Ritus,*Radiative corrections in quantum electrodynamics with intense fields and their analytical properties*, Ann. Phys. **69**, (1972) 555.

[16] G. Murguia, A. Raya, A. Sanchez, E. Reyes, *The electron propagator in external electromagnetic fields in lower dimensions*, Am. J. Phys. **78**, 700-707 (2010), arXiv:0910.1881 [hep-th].

[17] C. N. Leung, Y. J. Ng and A. W. Ackley, *Schwinger-Dyson equation approach to chiral symmetry breaking in an external magnetic field*, Phys. Rev. D **54**, 4181 (1996).

E. J. Ferrer and V. de la Incera, *Ward-Takahashi identity with external field in ladder QED*, Phys. Rev. D **58**, 065008 (1998), arXiv:hep-th/9803226.

C. N. Leung and S. -Y. Wang, *Gauge independent approach to chiral symmetry breaking in a strong magnetic field*, Nucl. Phys. B **747**, 266 (2006), arXiv:hep-ph/0510066.

[18] K. Fukushima, D. E. Kharzeev, H. J. Warringa, *Electric-current susceptibility and the chiral magnetic effect*, Nucl. Phys. **A836**, 311-336 (2010), arXiv:0912.2961 [hep-ph].

[19] C. Itzykson and J. B. Zuber, *Quantum Field Theory*, New York, USA: McGraw-Hill (1980).

[20] J. S. Schwinger, *On gauge invariance and vacuum polarization*, Phys. Rev. **82**, 664 (1951).

[21] E. J. Ferrer and V. de la Incera, *Dynamically induced Zeeman effect in massless QED*, Phys. Rev. Lett. **102**, 050402 (2009), arXiv:0807.4744 [hep-ph].

E. J. Ferrer and V. de la Incera, *Dynamically generated anomalous magnetic moment in massless QED*, Nucl. Phys. B **824**, 217 (2010), arXiv:0905.1733 [hep-ph].

[22] N. Sadooghi, *Chiral MHD description of a perfect*

magnetized QGP using the effective NJL model in a strong magnetic field, arXiv:0905.2097 [hep-ph].

[23] D. J. Bedingham, *Dimensional regularization and Mellin summation in high temperature calculations*, arXiv: hep-ph/0011012.

[24] E. J. Ferrer, V. de la Incera and A. Sanchez, *Paraelectricity in magnetized massless QED*, Phys. Rev. Lett. **107**, 041602 (2011), arXiv:1103.5152 [hep-ph].
E. J. Ferrer, V. de la Incera and A. Sanchez, *Non-perturbative Euler-Heisenberg Lagrangian and paraelectricity in magnetized massless QED*, arXiv:1204.3660 [hep-th].

[25] N. Sadooghi and K. S. Anaraki, *Improved ring potential of QED at finite temperature and in the presence of weak and strong magnetic field*, Phys. Rev. D **78**, 125019 (2008), arXiv:0805.0078 [hep-ph].

[26] D. E. Kharzeev, L. D. McLerran and H. J. Warringa, *The Effects of topological charge change in heavy ion collisions: 'Event by event P and CP violation'*, Nucl. Phys. **A803**, 227 (2008), arXiv:0711.0950 [hep-ph].
V. Skokov, A. Y. Illarionov and V. Toneev, *Estimate of the magnetic field strength in heavy-ion collisions*, Int. J. Mod. Phys. A **24**, 5925 (2009), arXiv:0907.1396 [nucl-th].

[27] V. de la Incera, *Nonperturbative physics in a magnetic field*, AIP Conf. Proc. **1361**, 74 (2011), arXiv:1004.4931 [hep-ph].
E. J. Ferrer, V. de la Incera, J. P. Keith, I. Portillo and P. P. Springsteen, *Equation of state of a dense and magnetized fermion system*, Phys. Rev. C **82**, 065802 (2010), arXiv:1009.3521 [hep-ph].

[28] B. Feng, E. J. Ferrer and V. de la Incera, *Magnetoelectric effect in strongly magnetized color superconductivity*, Phys. Lett. B **706**, 232 (2011), arXiv:1109.3100 [nucl-th].
B. Feng, E. J. Ferrer and V. de la Incera, *Photon self-energy and electric susceptibility in a magnetized three-flavor color superconductor*, arXiv:1203.1630 [hep-th].